Integrative analyses of metabolome and genome-wide transcriptome reveal the regulatory network governing flavor formation in kiwifruit (*Actinidia chinensis*)

Ruochen Wang[1]*, Peng Shu[1]*, Chi Zhang[2]*, Junlin Zhang[1], Ya Chen[1], Yaoxin Zhang[1], Kui Du[3], Yue Xie[3], Mingzhang Li[3], Tao Ma[1] (iD), Yang Zhang[1] (iD), Zhengguo Li[4] (iD), Don Grierson[5] (iD), Julien Pirrello[6], Kunsong Chen[2], Mondher Bouzayen[6] (iD), Bo Zhang[2] (iD) and Mingchun Liu[1] (iD)

[1]Key Laboratory of Bio-Resource and Eco-Environment of Ministry of Education, College of Life Sciences, Sichuan University, Chengdu 610065, China; [2]College of Agriculture & Biotechnology/Zhejiang Provincial Key Laboratory of Horticultural Plant Integrative Biology, Zhejiang University, Zijingang Campus, Hangzhou 310058, China; [3]Key Laboratory of Breeding and Utilization of Kiwifruit in Sichuan Province, Sichuan Provincial Academy of Natural Resource Sciences, Chengdu 610015, China; [4]Key Laboratory of Plant Hormones and Development Regulation of Chongqing, School of Life Sciences, Chongqing University, Chongqing 405200, China; [5]School of Biosciences, University of Nottingham, Sutton Bonington Campus, Loughborough, LE12 5RD, UK; [6]GBF Laboratory, Université de Toulouse, INRA, Castanet-Tolosan 31320, France

Authors for correspondence:
Mingchun Liu
Email: mcliu@scu.edu.cn

Bo Zhang
Email: bozhang@zju.edu.cn

Summary

- Soluble sugars, organic acids and volatiles are important components that determine unique fruit flavor and consumer preferences. However, the metabolic dynamics and underlying regulatory networks that modulate overall flavor formation during fruit development and ripening remain largely unknown for most fruit species.
- In this study, by integrating flavor-associated metabolism and transcriptome data from 12 fruit developmental and ripening stages of *Actinidia chinensis* cv Hongyang, we generated a global map of changes in the flavor-related metabolites throughout development and ripening of kiwifruit.
- Using this dataset, we constructed complex regulatory networks allowing to identify key structural genes and transcription factors that regulate the metabolism of soluble sugars, organic acids and important volatiles in kiwifruit. Moreover, our study revealed the regulatory mechanism involving key transcription factors regulating flavor metabolism. The modulation of flavor metabolism by the identified key transcription factors was confirmed in different kiwifruit species providing the proof of concept that our dataset provides a suitable tool for clarification of the regulatory factors controlling flavor biosynthetic pathways that have not been previously illuminated.
- Overall, in addition to providing new insight into the metabolic regulation of flavor during fruit development and ripening, the outcome of our study establishes a foundation for flavor improvement in kiwifruit.

Introduction

Fruit flavor is one of the most important quality attributes that influence consumer preference and market competitiveness. However, intensive breeding over the past half century has focused mainly on fruit yield and disease resistance rather than flavor traits and consumers have the perception that commercially produced fruits have lost their characteristic flavors (Klee & Tieman, 2013; Klee & Tieman, 2018). A possible solution to recover lost flavor is to conduct molecular breeding targeting flavor-regulating genes. However, the flavor phenotype is not always easy to measure quantitatively and is highly affected by the environment, therefore, the key genes involved in flavor metabolic regulation and the underlying mechanisms governing their expression have to date not been well defined.

Fruit flavor involves a complex set of interactions between taste and olfactory sensing (Tieman *et al.*, 2017). For most common fruits, taste is mainly determined by soluble sugars such as sucrose, glucose and fructose and organic acids including citrate and malate, while a diverse set of volatile compounds also provide particular olfactory stimuli conferring unique characteristics. Over the past decades, integration of multi-omics data such as metabolomics and transcriptomics, applied to the model plant tomato, has proven to be an excellent way to analyze flavor metabolic pathways and identify regulatory genes. For example, factors regulating the metabolism of soluble sugars and organic

---

*These authors contributed equally to this work.

acids during fruit development and ripening have been revealed through the combination of metabolic profiling and transcriptomic analysis in tomato (Carrari *et al.*, 2006). Osorio *et al.* (2012) using combined gas chromatography-mass spectrometry (GC-MS) and microarray-based analysis throughout fruit development and ripening to uncover different primary metabolic regulatory networks in tomato and pepper. Moreover, integration of the flavor metabolome and transcriptome with DNA methylome analysis, paved the way for the elucidation of the molecular mechanisms underlying the loss of tomato fruit flavor caused by chilling (Zhang *et al.*, 2016). Recently, genetic loci that affect tomato sugars, organic acids and flavor-related volatiles have been identified through the generation and analysis of large datasets that encompass genomes, transcriptomes, and metabolomes from hundreds of tomato accessions (Tieman *et al.*, 2017; Zhao *et al.*, 2019). Whereas the flavor-associated metabolism and key regulatory genes have been well studied in the fruit research model tomato, those regulating the accumulation of flavor-associated metabolites in other economically important fruits such as kiwifruit remain largely unknown. This knowledge is critical for understanding key biochemical pathways and identifying the structural and regulatory genes involved in the accumulation of sugars, acids and the production of unique volatiles in different fruits.

The kiwifruit (*Actinidia chinensis*) is an economically important fruit crop which originated in China and now has a global distribution (Huang *et al.*, 2013). Because of its distinctive flavor and high content of vitamins, minerals, amino acids and other metabolites recognized as beneficial to human health, kiwifruit has become one of the most popular fruits worldwide. Change in soluble sugars, organic acids, or volatiles during fruit development that affect fruit flavor have been widely studied in different kiwifruit species. These studies mainly focused on the flavor chemicals themselves, and on the identification of key enzymes and relevant biosynthesis genes during fruit development and ripening. For example, it has been shown that starch is degraded to glucose during the kiwifruit ripening process, and α-amylase (AMY) and β-amylase (BAM) were reported to be the key genes involved in starch degradation and sugar production (Zeeman *et al.*, 2010). In addition, sucrose synthase (SUS), sucrose phosphate synthetase (SPS), invertases (INV), hexokinase (HK) and fructokinase (FK) have also been identified as being involved in sugar metabolism in kiwifruit (Fung *et al.*, 2003; Richardson *et al.*, 2004; Moscatello *et al.*, 2011; Nardozza *et al.*, 2013). Previous studies have revealed that quinic acid, malic acid and citric acid are the main organic acids in kiwifruit (Sanz *et al.*, 2004; Nishiyama *et al.*, 2008). Quinic acid is one of the most important organic acids in different kiwifruit species and its high content confers a specific characteristic on fresh kiwifruit (Nishiyama *et al.*, 2008). It has been shown that quinic acid is a side product of the shikimic acid pathway and quinate dehydrogenase (QDH) genes have been suggested to play an important role in quinic acid biosynthesis (Marsh *et al.*, 2009). In addition to soluble sugars and organic acids, volatiles contribute one of the most important flavor determinants in kiwifruit. The main volatile substances in fruits include esters, alcohols, aldehydes, and

terpenes (Atkinson *et al.*, 2011; Garcia *et al.*, 2011; Zhang *et al.*, 2016). Esters such as ethyl butanoate and methyl butanoate, which are synthesized by alcohol acyltransferases (AATs), are the characteristic volatile aromatic compounds of ripe fruit in different kiwifruit species (Gunther *et al.*, 2010; Gunther *et al.*, 2011; Gunther *et al.*, 2015; Zhang *et al.*, 2020). However, so far little is known about the metabolic regulation and accumulation of soluble sugars, organic acids and volatiles in kiwifruit.

Recently, Zhang *et al.* (2018) identified by transcriptome coexpression network analysis a zinc finger protein, AdDof3, that modulates degradation of stored starch via regulation of *AdBAM3L* in kiwifruit. Using a similar approach, Zhang *et al.* (2020) generated a regulatory network of total esters and identified two transcription factors AdNAC5 and AdDof4 as key regulators modulating the expression of *AdFAD1*, a structural gene involved in kiwifruit ester biosynthesis. To date, however, there has been little research on the integration of flavor metabolism and transcriptome data to investigate the regulatory mechanisms underpinning flavor generation throughout kiwifruit development and ripening.

In this study, we investigated the metabolic dynamics of flavor and the regulatory mechanisms underlying flavor generation during kiwifruit development and ripening. We selected six developmental (40, 60, 80, 100, 120 and 140 DAP (days after pollination)) and six ripening stages (4, 6, 8, 10, 12 and 14 DAH (days after harvest) of ripening fruit) of 'Hongyang' kiwifruit. Through a combination of flavor-associated metabolite studies and transcriptome analysis, we constructed a regulatory network controlling production and accumulation of soluble sugars, organic acids and volatiles. In addition, we identified key transcription factors that modulate flavor metabolism via direct transcriptional regulation of their structural gene targets. Overall, our study provides new insights into the regulation of flavor metabolism and establishes a foundation for flavor improvement in kiwifruit.

Materials and Methods

Plant material and measurements

Kiwifruit (*Actinidia chinensis* cv Hongyang) at different developmental stages were collected from a farm in Shifang, Sichuan province, China. Fruits at different developmental stages were collected from 40 DAP to 140 DAP including 40, 60, 80, 100, 120 and 140 DAP. Fruits harvested at 140 DAP were stored at room temperature and sampled from 4 to 14 DAH to represent different ripening stages (4, 6, 8, 10, 12 and 14 DAH). The outer pericarp (without skin and seeds) of the fruit was cut into small pieces and rapidly frozen in liquid nitrogen and then stored at −80°C for further metabolic and transcriptomic analysis. All experiments were analyzed with three biological repeats and each repeat consisted of 15 fruits of uniform size.

Fruit weight, soluble solids concentration (SSC), firmness and ethylene production were measured throughout fruit development and ripening. SSC were measured using a digital hand-held refractometer (Atago, Tokyo, Japan) by placing a drop of the

supernatant of mashed fruit on a refractometer and the values recorded. Firmness was measured using a TA.XT plus texture analyzer (Stable Microsystems, Godalming, UK) with three replicates (six fruit in each replicate) for each stage, following a method described previously (Deng *et al.*, 2018). Ethylene was measured with a GC1120 gas chromatograph (Sunny Hengping, Shanghai, China), using the detailed parameters described previously (Deng *et al.*, 2018). Measurements were made at each stage with three biological replicates and six fruits in each replicate.

Flavor-related metabolic analysis

Soluble sugars and organic acids were analyzed according to the method described (Zhang *et al.*, 2020). Frozen kiwifruit samples (100 mg) were extracted with 1.4 ml methanol at 70°C for 15 min, and then centrifuged at 11 000 *g* for 10 min. Next, 10 µl ribitol was added as an internal standard. After 3 h drying, the residue was dissolved in 60 µl of 20 g l^{-1} pyridine methoxyamine hydrochloride, and incubated at 37°C for 1.5 h. The sample was then treated with 40 µl *N,O*-bis(trimethylsilyl)trifluoroacetamide (BSTFA) at 37°C for 0.5 h. Then, 1 µl aliquots of each sample were absorbed with a split ratio of 10 : 1 and injected into an Agilent 6890 N gas chromatograph (Agilent, Palo Alto, CA, USA) fitted with an HP-5 column (30 m, 0.25 mm, 0.25 µm; Agilent). Nitrogen was used as a carrier gas. The temperature of the quadrupole was 150°C, the injector was 250°C, and the detector was 280°C. Chromatography conditions were as follows: initial oven temperature, 100°C, held for 1 min, increased by 2.5°C min^{-1} to 185°C, increased by 10°C min^{-1} to 250°C, and held for 1 min, increased by 5°C min^{-1} to 280°C, and held for 3 min. The sugars and acids analyses were performed using three biological replicates. Volatiles were analyzed by a headspace, solid-phase microextraction, and gas chromatography-mass spectrometry (HS-SPME-GC-MS) system according to the method described previously (Zhang *et al.*, 2009) with minor modifications. Frozen kiwifruit samples (5.0 g) were mixed with 5 ml saturated sodium chloride (NaCl) solution and the internal standard (2-octanol). After 30 min equilibration, volatiles were collected using fibers coated with 65 µm of polydimethylsiloxane and divinylbenzene (PDMS-DVB, Supeclo, Bellefonte, PA, USA) and then separated by a DB-Wax column (0.32 mm, 30 m, 0.25 µm; Agilent). Chromatograph conditions were as follows: injector, 220°C; initial oven temperature, 34°C, held for 2 min, increased by 2°C min^{-1} to 60°C, then increased by 4°C min^{-1} to 180°C, and held for 2 min. Volatiles were identified by comparing with the mass spectra of the NIST Mass Spectral Library (NIST-08) and comparison of retention time of authentic standards. Quantification of compounds was performed using the peak area of the internal standard as a reference based on total ion chromatogram (TIC). The volatile analysis was performed with three biological replicates.

RNA sequencing and data analysis

Total RNA was extracted from frozen fruits and messenger RNA (mRNA) libraries were constructed for each sample and sequenced using the Illumina HiSeq-2000 platform. For data analysis, paired reads were mapped to the *Actinidia chinensis* (Red5_PS1_1.69.0, https://plants.ensembl.org/Actinidia_chinensis) genome assembly using HISAT 2 with default parameters (Kim *et al.*, 2015). Uniquely mapped reads with MAPQ > 20 were collected for further analysis. The mapped fragments for each gene were counted by featureCounts (Liao *et al.*, 2014) and transcripts per million (TPM) were calculated. Genes with averaged TPM (replicates = 3) were considered expressed. Principal component analysis (PCA) was performed to compare the TPM values of the expressed gene profiles among development and ripening stages using the PRCOMP function in R. Hierarchical clustering and heatmaps of expressed genes were generated using the PHEATMAP packages in R.

Weighted correlation network analysis and gene network visualization

After discarding undetectable or relative low expression genes (TPM < 10), differentially expressed genes (DEGs) (coefficient of variation (CV) > 0.5) were used to generate co-expression network modules by weighted gene co-expression network analysis (WGCNA) package in R. The co-expression modules were obtained using automatic network construction function (blockwiseModules) with default parameters, apart from the soft threshold power of 26, TOMtype was signed, mergeCutHeight was 0.25 and minModuleSize was 100. The initial clusters were merged on eigengenes. Eigengene value was calculated for each module, which was used to search the association with flavor substances (sugars, acids, volatiles) produced during fruit development and ripening. The position frequency matrices (PFMs) of transcription factors were obtained from plantTFDB (Jin *et al.*, 2017), which were used to predict *cis*-acting element information in the promoter region of the structural genes (1000 bp upstream and 200 bp downstream of the transcription start site) under the condition of *P* value $\leq$ 1e^{-4} by FIMO (Grant *et al.*, 2011). The transcriptional regulatory networks were generated by combining the Pearson correlation coefficient (PCC > 0.8) between structural genes and transcription factors and the availability of *cis*-element binding sites present in the promoter regions of structural genes in the same module. The networks were visualized by CYTOSCAPE (v.3.7.2, USA) (Kohl *et al.*, 2011).

Real-time quantitative polymerase chain reaction analysis

Total RNA from fruit at different development and ripening stages was isolated using a Plant RNA Purification Reagent (Invitrogen, Carlsbad, CA, USA) according to the manufacturer's instructions. Genomic DNA contamination treatment, first-strand complementary DNA generation and real-time quantitative polymerase chain reaction (RT-qPCR) analysis was carried out in accordance with the described protocols (Deng *et al.*, 2018) RT-qPCR was performed using the CFX384 Touch Real-Time PCR Detection System (Bio-Rad, Hercules, CA, USA). Three biological replicates were analyzed with the kiwifruit *Actin*

gene as an internal control. The primers for RT-qPCR are listed in Supporting Information Table S1.

Transient dual luciferase reporter assays

Full-length coding sequences of *AcERF182* and *AcNAC4* were cloned into pGreen II 62-SK vector to generate the effectors, while the promoter sequences of *AcBAM3.5* and *AcAAT10* were cloned into the pGreen II 0800-LUC double-reporter vector. The constructed reporter and effector plasmids were then transferred into tobacco protoplasts by polyethylene glycol-mediated transfection. Firefly and renilla luciferase were assayed with the Dual-Luciferase Reporter Assay System (Promega, Madison, WI, USA) as described by Ying *et al.* (2020). The empty pGreen II 62-SK vector was used as the control. The results are presented as the ratio of LUC to REN activity from three independent biological replicates. Primers used for vector construction are listed in Table S1.

Yeast one-hybrid assay

The yeast one-hybrid (Y1H) assays were conducted based on the method previously described (Ying *et al.*, 2020). Three tandem copies of the *AcBAM3.5* and *AcAAT10* promoter sequences containing the core *cis*-elements were synthesized and then inserted into pHis2-Leu-GW vectors. The recombinant vectors were then transformed into the yeast strain Y187 cells by the lithium chloride-polyethylene glycol (LiCl-PEG) method according to the manufacturer's manual (Clontech, Mountain View, CA, USA). The full-length coding sequences of *AcERF182* and *AcNAC4* were amplified and inserted into pDEST22 vectors and transformed into yeast strains containing pHis2-Leu-*AcBAM3.5* or pHis2-Leu-*AcAAT10*. The empty pDEST22 vector was used as the control. The transformants were further grown on SD/-Leu/-Trp medium. Finally, positive yeast clones were cultivated in SD/-Leu/-Trp liquid medium and diluted to different concentrations (optical density at 600 nm (OD_{600}) = 1, 10^{-1}, 10^{-2} and 10^{-3}), and 2.5 μl yeast suspension was plated on the SD/-Leu/-Trp/-His medium with 0 mM and 10 mM 3-AT (3-amino-1,2,4-triazole).

Electrophoretic mobility shift assay

The full-length coding sequence of *AcERF182* and *AcNAC4* were amplified and inserted into the pGEX4T-1 vector to generate GST fusion proteins. The purification of *AcERF182*-GST and *AcNAC4*-GST was conducted using the GST Sefinose Resin (Sangon Biotech, Shanghai, China) for use in further electrophoretic mobility shift assay (EMSA) experiments. The 40 bp probes of the promoters containing the putative *cis*-elements binding sites of corresponding target genes were labeled with biotin at the 3′ end with Biotin 3′ End DNA Labeling Kit (Thermo Scientific, Waltham, MA, USA) according to the manufacturer's directions. EMSA was conducted using a LightShift Chemiluminescent EMSA Kit (Thermo Scientific). Mutant probes and cold probes (200-fold concentration of unlabeled oligonucleotides) were utilized for competition experiments in EMSA.

Transient overexpression or silencing of transcription factor genes in fruit

To generate *AcERF182* and *AcNAC4* overexpression constructs in fruit of 'Hongyang', the coding sequence of the two transcription factors were amplified with primers listed in Table S1. The purified PCR products were recombined into pBI121 vector with double digestions and transformed into *Agrobacterium tumefaciens* strain (GV3101), separately. To generate the virus-induced gene silencing (VIGS)-mediated *AcERF182* and *AcNAC4* silenced lines, partial coding sequences of *AcERF182* and *AcNAC4* were cloned and ligated into pTRV2 vector with primers listed in Table S1. pTRV2-*AcERF182*, pTRV2-*AcNAC4* and pTRV1 were transformed into *Agrobacterium tumefaciens* strain (GV3101) separately. The infiltration mix was injected into on-vine fruits at a depth of 0.5 cm at 100 DAP with the empty vector as a control. To ensure the best efficiency of transient expression, we continued to perform injections every 10 d before collecting the sample. For each fruit, three sites were injected and six biological replications were performed. The outer pericarp (without skin or seeds) of kiwifruit was collected at 140 DAP and rapidly frozen with liquid nitrogen and then stored at −80°C for further analysis.

Accession numbers

The raw RNA-sequencing (RNA-Seq) data has been submitted to the Genome Sequence Archive in National Genomics Data Center, Beijing Institute of Genomics, Chinese Academy of Sciences. The accession number is CRA003106 and is publicly accessible at http://bigd.big.ac.cn/.

Results

Flavor-associated metabolic profiling during fruit development and ripening of *Actinidia chinensis* cv Hongyang

To investigate the flavor-associated metabolic regulatory network during kiwifruit developmental and ripening processes, 12 stages including six developmental stages (40, 60, 80, 100, 120 and 140 DAP) and six ripening stages (4, 6, 8, 10, 12 and 14 DAH) of *Actinidia chinensis* cv Hongyang were selected (Fig. 1a). Kiwifruit harvested at 140 DAP and then stored at 20°C for up to 14 d were taken as ripening stages. Because kiwifruit is a typical climacteric fruit extremely perishable if picked at full-ripe stage, the common commercial practice is to harvest the fruits at physiological mature stage (140 DAP for Hongyang) and then to store them for postharvest ripening. Therefore, in line with our objective to characterize the flavors of the fruit that are of interest to consumers and in an attempt to mimic the normal commercialization practice, the fruits were picked at 140 DAP and then stored for postharvest ripening. During the developmental stages,
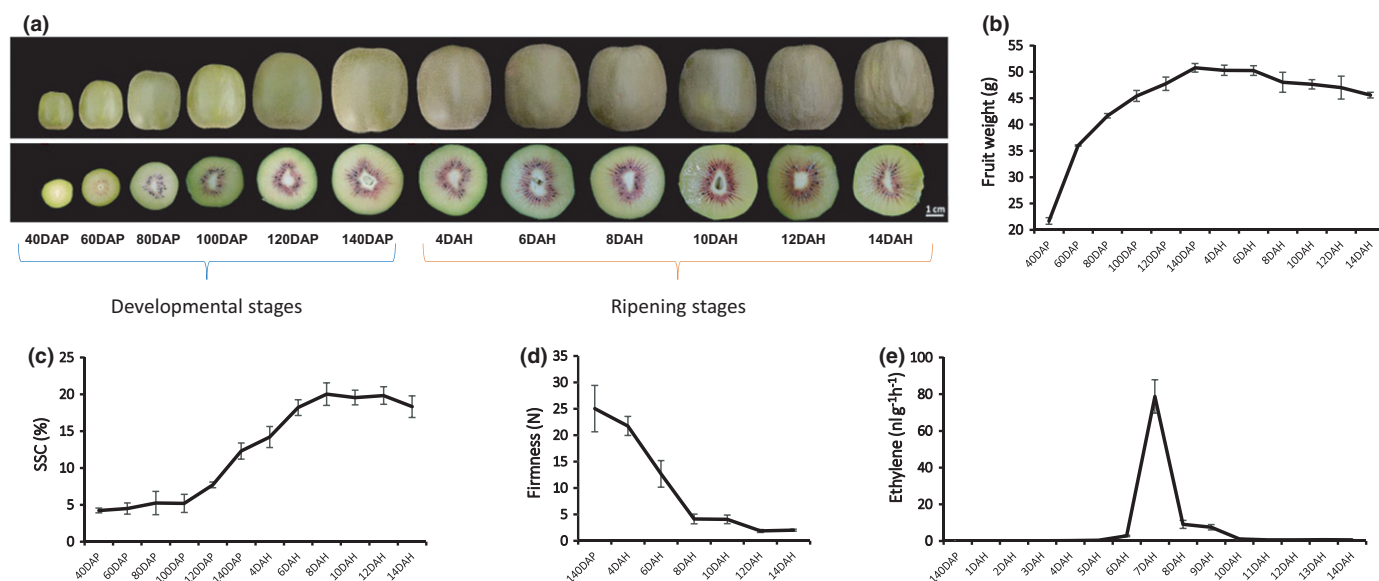
Fig. 1 Twelve fruit developmental and ripening stages selected for analysis in kwifruit. (a) Six developmental and six ripening stages of *Actinidia chinensis* cv Hongyang. DAP, days after pollination; DAH, days after harvest at 140 DAP. Bar, 1 cm. (b) Fruit weight during fruit development and ripening from 40 DAP to 14 DAH in Hongyang. (c) Soluble solids concentration (SSC) during kiwifruit development and ripening. A total of 15 fruits were used for each measurement and the values shown are the means ± SD. (d) Fruit firmness during fruit ripening including 140 DAP (harvest), 4 DAH, 6 DAH, 8 DAH, 10 DAH, 12 DAH and 14 DAH. (e) Ethylene production during fruit ripening from 140 DAP (harvest) to 14 DAH in *Actinidia chinensis* cv Hongyang.

a rapid increase of fruit weight was observed from 40 to 80 DAP, then the increase continued at a moderate pace peaking at 140 DAP (Fig. 1b). The SSC of kiwifruit gradually increased and reached a peak of 20.02% at 8 DAH (Fig. 1c). By contrast, the fruit firmness decreased during ripening, with a sharp decrease from 4 to 8 DAH (Fig. 1d), indicating that kiwifruit reached the accepted edible ripening stage at 8 DAH. Moreover, climacteric ethylene production peaked at 7 DAH (Fig. 1e), which is consistent with the timing of the change in firmness during ripening.

Soluble sugars, organic acids and volatiles are the main contributors to the unique flavor of kiwifruit. To investigate the flavor dynamics throughout kiwifruit development and ripening, we monitored the changes in soluble sugars and organic acids by GC and volatiles using a GC-MS-based metabolic profiling method. A total of 34 flavor-associated metabolites were identified, including three soluble sugars, three organic acids and 28 volatiles (Fig. 2a; Tables 1, 2). Based on their accumulation at different developmental and ripening stages, these metabolites were divided into two groups (Fig. 2a). Metabolites in group I included ethyl butanoate, ethyl benzoate, ethyl valerate, ethyl caproate, citric acid, sucrose, fructose, glucose, methyl butanoate and methyl benzoate, which accumulated preferentially during fruit ripening (Fig. 2a). These metabolites likely account for the typical flavor of ripe kiwifruit. Metabolites in group II including various aldehydes, alcohols, ketones and two organic acids, which represent the main flavor components of unripe fruit, accumulate mainly during developmental stages before ripening (Fig. 2a). These results indicate that the typical flavors present during the developmental and ripening stages are different and there is a shift in the composition of volatiles from aldehydes, alcohols, ketones in developmental stages to esters in ripening stages. PCA

confirmed that these flavor-associated metabolites could be divided into two groups associated with either the developmental or ripening stages (Fig. 2b). Accordingly, the cluster dendrogram also distinguished two groups (Fig. 2b) which is consistent with the PCA. All these results revealed that the accumulation of flavor-associated metabolites is stage-specific during fruit development and ripening processes in kiwifruit.

Genetic basis of dynamic changes in flavor metabolites during fruit development and ripening of *Actinidia chinensis* cv Hongyang

To investigate the genetic basis of flavor-associated metabolism over the course of kiwifruit development and ripening, RNA-Seq data were generated for 12 different developmental and ripening stages. After removing adapter reads, ambiguous reads and low-quality reads, 6.57 Gb clean reads on average were produced (Supporting Information Dataset S1). The expression levels indicated by TPM reads showed high correlations between biological replicates (Dataset S2). In total, 23 168 genes were found to be expressed (averaged TPM ≥ 1, median absolute deviation ≥ 0.01) in 12 different developmental and ripening stages (Dataset S3). Based on the expression pattern during fruit developmental and ripening stages, these genes could also be divided into two groups (Fig. 2c; Dataset S4) as found for the accumulation pattern of flavor-associated metabolites. Group I genes (32%, 7342 out of 23 168) were specifically expressed during fruit ripening stages (Fig. 2c), whereas group II genes (68%, 15 826 of 23 168) were mainly expressed during stages of fruit development before ripening (Fig. 2c). The PCA and cluster dendrogram of the transcriptome also supported the classification of gene expression patterns
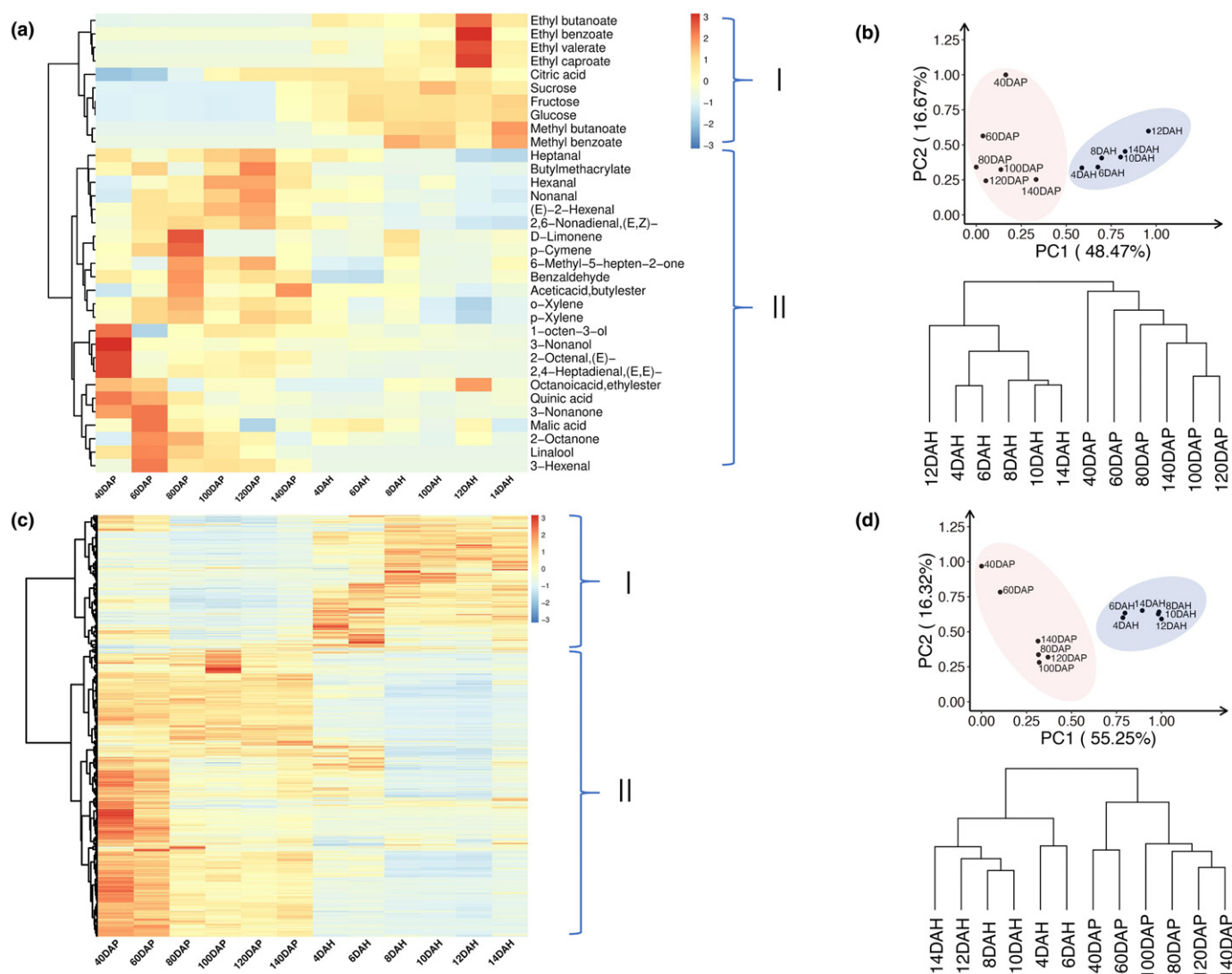
Fig. 2 Flavor-related metabolome and transcriptome data analysis in kwifruit. (a) Overview of flavor-related metabolome throughout fruit developmental and ripening stages of *Actinidia chinensis* cv Hongyang. Metabolites in Clade I accumulate during fruit ripening; Metabolites in Clade II accumulate during fruit developmental stages. DAP, days after pollination; DAH, days after harvest at 140 DAP. (b) Principal component analysis (PCA) and cluster dendrogram of metabolome data from 12 developmental and ripening stages of *Actinidia chinensis* cv Hongyang. (c) Transcriptomic data are divided into two clades during kiwifruit development and ripening. Genes in group I are highly expressed during fruit ripening; Genes in group II are highly expressed during fruit developmental stages. (d) PCA and cluster dendrogram of transcriptomic data from 12 developmental and ripening samples of *Actinidia chinensis* cv Hongyang.

into two groups (Fig. 2d). Overall, both the metabolome and transcriptome showed significant developmental specificity during different stages of fruit development and ripening in *Actinidia chinensis* cv Hongyang.

To gain further insight into the regulation of the metabolic changes throughout kiwifruit development and ripening, weighted gene co-expression network analysis (WGCNA) was performed to investigate the co-expression networks of DEGs. A total of 10 co-expression modules were identified based on their similar expression patterns (Fig. 3a; Dataset S5). Genes preferentially expressed during fruit ripening were mainly gathered in the blue module, while most of the genes highly expressed during fruit development processes were located in turquoise and yellow

modules (Fig. 3a; Dataset S5). The heatmap of module-trait correlations (Fig. 3b) indicated that the accumulation of transcripts for the blue module was correlated with flavor-associated metabolites including sucrose, fructose, glucose, ethyl butanoate, and methyl butanoate, which preferentially accumulated during fruit ripening. However, the accumulation of transcripts in turquoise and yellow modules were correlated with flavor-associated metabolites such as (*E*)-2- hexenal, hexanal, linalool, and quinic acid, which are present as the main flavor compounds of kiwifruit at different developmental stages before ripening. These results indicate that genes in these three modules are mainly associated with flavor changes during fruit development and ripening of *Actinidia chinensis* cv Hongyang.

Table 1 Content of sugars and organic acids at different developmental and ripening stages in 'Hongyang' kiwifruit (mg g^{-1}) and the values shown are the means ± SD.

	40 DAP	60 DAP	80 DAP	100 DAP	120 DAP	140 DAP	4 DAH	6 DAH	8 DAH	10 DAH	12 DAH	14 DAH
Fructose	1.7 ± 0.2	2.0 ± 0.0	1.7 ± 0.2	0.7 ± 0.1	1.6 ± 0.2	19.9 ± 1.5	25.6 ± 2.6	39.7 ± 1.3	36.2 ± 0.4	36.9 ± 0.1	34.6 ± 2.4	41.4 ± 0.3
Glucose	1.5 ± 0.1	1.6 ± 0.1	1.3 ± 0.2	0.5 ± 0.1	1.4 ± 0.2	18.9 ± 1.4	25.1 ± 2.6	39.5 ± 0.9	36.2 ± 0.3	36.9 ± 0.2	33.6 ± 2.9	39.3 ± 0.3
Sucrose	2.5 ± 0.5	1.1 ± 0.1	1.4 ± 0.0	1.4 ± 0.2	1.8 ± 0.1	27.0 ± 3.0	35.5 ± 4.3	47.0 ± 1.9	46.4 ± 0.6	60.0 ± 1.3	48.9 ± 2.6	38.5 ± 0.2
Malic acid	2.2 ± 0.1	3.4 ± 0.1	2.5 ± 0.2	2.3 ± 0.1	1.5 ± 0.1	2.1 ± 0.1	2.4 ± 2.2	2.6 ± 0.0	2.2 ± 0.1	1.9 ± 0.1	2.4 ± 0.1	1.7 ± 0.0
Citric acid	0.0 ± 0.1	0.5 ± 0.0	2.7 ± 0.2	5.6 ± 0.2	6.9 ± 0.3	6.9 ± 0.3	7.3 ± 0.4	7.2 ± 0.3	6.4 ± 0.3	5.6 ± 0.2	6.9 ± 0.3	5.2 ± 0.2
Quinic acid	19.7 ± 1.9	17.5 ± 0.4	13.6 ± 0.9	9.6 ± 0.3	10.8 ± 0.1	10.1 ± 0.5	8.7 ± 0.5	8.6 ± 0.3	9.9 ± 0.1	8.5 ± 0.1	9.5 ± 0.4	10.0 ± 0.3

DAP, days after pollination; DAH, days after harvest at 140 DAP.

Generation of flavor metabolic regulatory networks

Soluble sugars are among the most important components contributing to the characteristic flavor of kiwifruit. Interestingly, and the accumulation of sucrose, fructose, glucose was highly correlated with the blue module (Fig. 3b). To generate the regulatory network associated with soluble sugars metabolism, we examined the structural genes involved in soluble sugar metabolic pathway identified in the blue module (Fig. 4a). We identified 21 soluble sugar-metabolizing genes including five *invertases* (*INV*), two *sucrose synthases* (*SUS*), two *hexokinases* (*HK*), six α-/ß-*amylases* (*AMY/BAM*), two *fructokinases* (*FK*), one *ADP glucose pyrophosphorylase* (*AGPase*), and three *sucrose phosphate synthetases* (*SPS*) genes in the blue module (Fig. 4a; Dataset S6) whose expression was highly correlated with the accumulation of the three soluble sugars. By correlating the patterns of transcript accumulation and the potential binding affinity for the promoters of metabolic structural genes associated with the biosynthesis of soluble sugar, we identified 92 transcription factors including ERF, NAC, MYB and bHLH whose expression was highly correlated with the 21 soluble sugar-metabolizing structural genes in the blue module and formed a correlation network (Fig. 4a; Dataset S6). This suggested that these transcription factors correspond to the putative regulators controlling soluble sugar metabolism during fruit ripening.

Organic acids including quinic acid, citric acid, and malic acid play a vital role in the formation of typical kiwifruit flavor. Quinic acid is the major organic acid of many *Actinidia* species and is a unique fresh fruit flavor component in kiwifruit, including the 'Hongyang' cultivar. Quinic acid is a side product of the shikimic acid pathway (Marsh *et al.*, 2009) and *3-deoxy-D-arabino-heptulosonate 7-phosphate synthase* (*DAHPS*), *3-dehydroquinate synthase* (*DHQS*), and *quinate dehydrogenase* (*QDH*) are the putative structural genes involved in the biosynthesis of quinic acid (Fig. 4b). To identify the key regulators controlling quinic acid metabolism, we firstly examined the key structural genes involved in the quinic acid biosynthesis pathway in the turquoise module which were highly correlated with quinic acid accumulation. We identified five structural genes including four *DAHPSs* (*AcDAHPS1, AcDAHPS2, AcDAHPS5, AcDAHPS6*) and one *QDH* (*AcQDH4*) in the turquoise module (Fig. 4b) whose transcripts were highly correlated with quinic acid content throughout fruit development and ripening. To further characterize the transcription factors that putatively regulate quinic acid metabolism, we screened 83 transcription factors including MYB, ERF, NAC, bHLH families in the turquoise module and constructed a regulation network (Fig. 4b) by combining expression correlation and the binding ability to the *cis*-elements present in the promoter regions of these structural genes (Dataset S7).

The aroma of kiwifruit results from a subtle mixture of volatile compounds and is a crucial factor for consumer acceptance (Marsh *et al.*, 2006). Since esters such as ethyl butanoate and methyl butanoate are the most important contributors to the fruity aroma of ripe kiwifruit, we attempted to generate the regulatory network associated with the metabolism of the two compounds. To date, the metabolic pathway of ethyl butanoate and methyl butanoate in kiwifruit remains unclear. Given the structure of the two esters, we speculated that the β-oxidation

Table 2 Content of volatile compounds at different developmental and ripening stages in 'Hongyang' kiwifruit (ng g^{-1}) and the values shown are the means ± SD.

Volatile compounds	40 DAP	60 DAP	80 DAP	100 DAP	120 DAP	140 DAP	4 DAH	6 DAH	8 DAH	10 DAH	12 DAH	14 DAH
Terpenoids												
D-Limonene	3135.2 ± 747.9	6947.6 ± 160.7	16529.2 ± 2575.0	1014.1 ± 210.4	982.3 ± 157.9	3285.8 ± 542.4	1059.3 ± 60.1	1658.6 ± 604.4	8580.5 ± 1269.7	1330.5 ± 356.7	1757.2 ± 686.7	3317.6 ± 797.2
Linalool	771.4 ± 126.2	1408.7 ± 114.6	939.9 ± 84.5	765.5 ± 81.3	359.5 ± 14.2	108.7 ± 17.5	19.3 ± 2.9	19.7 ± 1.4	22.1 ± 2.9	19.5 ± 2.4	28.7 ± 4.7	17.8 ± 1.0
Alcohols												
3-Nonanol	33.5 ± 3.2	12.8 ± 1.0	12.5 ± 0.6	11.4 ± 1.1	13.3 ± 1.3	10.7 ± 1.1	10.4 ± 1.6	11.8 ± 2.1	11.8 ± 0.0	10.3 ± 0.9	10.2 ± 1.2	9.9 ± 1.9
1-Octen-3-ol	84.2 ± 7.0	9.4 ± 1.0	41.0 ± 11.0	54.7 ± 13.0	53.2 ± 8.1	42.7 ± 8.0	43.3 ± 2.0	34.0 ± 4.7	28.7 ± 2.4	33.3 ± 2.0	30.4 ± 1.8	28.3 ± 3.2
Ketones												
2-Octanone	99.7 ± 6.5	160.4 ± 1.0	152.4 ± 3.2	133.5 ± 2.8	127.7 ± 4.5	104.2 ± 3.5	119.9 ± 5.4	112.7 ± 3.2	110.0 ± 3.8	105.5 ± 2.7	121.2 ± 1.6	108.0 ± 3.5
6-Methyl-5-hepten-2-one	113.1 ± 13.0	68.2 ± 6.7	224.7 ± 5.6	163.3 ± 32.1	213.1 ± 14.9	118.2 ± 7.0	58.7 ± 6.4	51.9 ± 7.2	117.0 ± 3.6	84.5 ± 9.3	79.8 ± 0.1	125.0 ± 18.3
3-Nonanone	8.5 ± 2.5	9.9 ± 0.3	4.0 ± 0.9	3.2 ± 0.3	2.6 ± 0.4	2.0 ± 0.2	2.0 ± 0.1	2.2 ± 0.0	2.5 ± 0.2	2.0 ± 0.2	2.2 ± 0.4	2.1 ± 0.1
Aldehydes												
Hexanal	35.2 ± 5.5	188.1 ± 17.2	301.3 ± 67.3	517.9 ± 60.1	521.7 ± 53.5	351.8 ± 21.6	170.1 ± 1.5	208.3 ± 18.2	80.7 ± 6.1	196.2 ± 15.5	64.0 ± 7.3	37.0 ± 1.8
3-Hexenal	2.2 ± 0.4	36.6 ± 9.0	18.8 ± 4.3	20.7 ± 1.4	18.4 ± 1.7	7.2 ± 0.8	0.0	0.0	0.0	0.0	0.0	0.0
(E)-2-Hexenal	748.0 ± 144.1	1761.5 ± 84.8	1719.9 ± 275.0	2268.5 ± 139.9	2470.4 ± 150.6	994.7 ± 54.4	263.9 ± 12.2	354.2 ± 42.3	112.3 ± 11.0	469.2 ± 85.8	61.6 ± 4.5	29.4 ± 3.7
Nonanal	21.4 ± 2.3	64.8 ± 7.7	54.4 ± 10.2	71.7 ± 8.2	85.3 ± 6.9	48.4 ± 4.0	47.8 ± 3.1	45.9 ± 4.5	32.8 ± 1.7	30.2 ± 1.6	26.8 ± 3.2	21.0 ± 1.8
(E)-2-Octenal	330.4 ± 18.7	52.8 ± 8.5	90.2 ± 13.9	108.3 ± 25.2	137.6 ± 17.5	111.8 ± 3.1	43.9 ± 10.6	38.7 ± 1.6	31.4 ± 3.1	27.1 ± 1.3	29.2 ± 3.6	30.2 ± 6.4
(E,E)-2,4-Heptadienal	295.8 ± 8.4	52.9 ± 5.3	111.8 ± 0.6	99.7 ± 16.8	112.9 ± 32.7	57.2 ± 5.5	35.9 ± 6.3	22.5 ± 1.2	16.5 ± 1.6	32.4 ± 6.9	21.9 ± 0.5	21.4 ± 6.2
Benzaldehyde	95.6 ± 16.1	78.6 ± 5.8	137.4 ± 12.7	87.4 ± 2.7	107.4 ± 6.3	95.9 ± 4.8	34.5 ± 3.8	32.4 ± 3.1	69.1 ± 8.5	56.6 ± 5.1	57.6 ± 4.2	70.0 ± 4.9
(E,Z)-2,6-Nonadienal	10.9 ± 0.3	19.4 ± 0.5	21.4 ± 0.8	20.0 ± 1.8	24.3 ± 1.6	17.8 ± 2.7	14.4 ± 1.5	10.2 ± 1.8	7.5 ± 0.2	7.7 ± 0.5	5.3 ± 0.4	4.4 ± 1.1
Heptanal	9.9 ± 0.6	6.7 ± 0.9	8.9 ± 0.5	10.9 ± 1.7	11.9 ± 0.4	7.8 ± 0.5	9.0 ± 1.1	7.8 ± 0.4	5.8 ± 0.3	5.8 ± 0.5	3.7 ± 0.4	3.5 ± 0.6
Esters												
Aceticacid, butylester	9.1 ± 2.2	23.5 ± 0.9	54.5 ± 0.3	25.2 ± 1.6	29.5 ± 0.9	56.5 ± 9.1	27.0 ± 1.4	27.8 ± 0.2	28.0 ± 1.4	19.4 ± 1.2	12.0 ± 0.4	18.9 ± 1.4
Butyl methacrylate	6.1 ± 2.3	11.1 ± 1.2	1.3 ± 0.0	8.9 ± 0.7	16.1 ± 1.0	8.4 ± 1.1	1.3 ± 0.3	1.1 ± 0.1	0.8 ± 0.1	0.9 ± 0.0	0.0	0.5 ± 0.0
Octanoicacid, ethylester	66.3 ± 11.0	59.5 ± 16.4	0.0	22.3 ± 2.7	21.2 ± 6.1	0.0	0.0	0.0	23.3 ± 7.9	19.4 ± 3.4	76.3 ± 4.7	16.2 ± 2.8
Methyl butanoate	0.0	0.0	0.0	0.0	0.0	15.8 ± 2.1	47.8 ± 9.2	76.5 ± 6.0	129.5 ± 2.6	130.8 ± 32.3	85.2 ± 9.0	175.9 ± 46.3
Ethyl butanoate	26.2 ± 4.6	49.2 ± 2.4	94.9 ± 1.0	55.1 ± 4.3	72.0 ± 0.8	159.3 ± 19.8	2230.4 ± 141.3	1698.3 ± 80.8	1264.2 ± 17.6	2247.0 ± 355.9	5073.9 ± 306.6	2259.4 ± 178.8
Ethyl valerate	0.0	0.0	0.0	0.0	0.0	0.0	12.5 ± 1.8	2.9 ± 0.5	10.3 ± 0.1	16.8 ± 2.6	46.3 ± 10.0	15.2 ± 0.6
Ethyl caproate	7.2 ± 2.0	0.0	0.0	0.0	2.8 ± 0.3	0.0	32.8 ± 14.7	8.8 ± 3.8	343.3 ± 59.7	410.6 ± 72.0	1382.7 ± 260.7	356.1 ± 15.7
Methyl benzoate	0.0	0.0	0.0	0.0	0.0	5.3 ± 0.7	57.5 ± 29.9	67.7 ± 55.2	1960.6 ± 190.6	1683.7 ± 313.6	825.9 ± 70.6	2010.1 ± 96.1
Ethyl benzoate	4.4 ± 0.5	4.6 ± 0.8	6.4 ± 0.7	2.9 ± 0.4	0.0	2.5 ± 0.8	23.5 ± 16.8	3.7 ± 2.6	169.9 ± 5.2	370.5 ± 83.6	5557.8 ± 689.9	532.7 ± 63.9
Benzenoid compounds												
p-Xylene	17.8 ± 5.0	31 ± 6.0	32.8 ± 0.9	19.5 ± 1.7	31.8 ± 14.5	30.0 ± 2.9	18.7 ± 5.9	12.3 ± 0.9	17.5 ± 0.6	9.6 ± 1.9	5.2 ± 0.0	11.1 ± 3.1
o-Xylene	13.8 ± 5.0	21.3 ± 2.8	24.0 ± 1.2	16.8 ± 1.1	20.1 ± 8.2	17.4 ± 2.4	14.3 ± 5.7	8.4 ± 0.4	13.3 ± 0.6	7.2 ± 1.1	3.8 ± 0.1	8.5 ± 2.3
p-Cymene	180.0 ± 28.0	392.3 ± 40.2	621.6 ± 51.5	57.2 ± 10.1	58.9 ± 6.5	182.5 ± 17.2	59.5 ± 5.9	82.2 ± 15.7	292.3 ± 38.5	57.0 ± 12.6	66.0 ± 21.8	130.0 ± 31.4

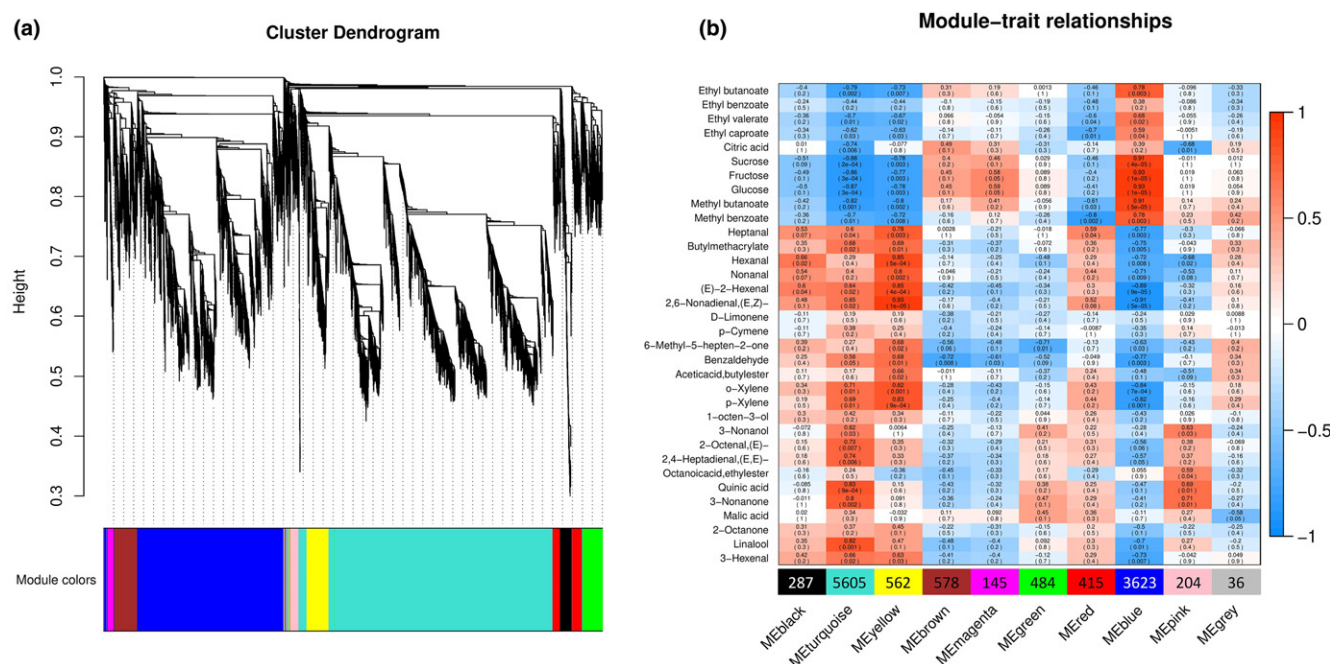DAP, days after pollination; DAH, days after harvest at 140 DAP.

Fig. 3 Transcriptomic and metabolic correlation analysis across fruit developmental and ripening stages in kiwifruit. (a) Dendrogram showing co-expression modules (clusters) identified by weighted correlation network analysis (WGCNA) across fruit developmental and ripening stages. The major tree branches constitute 10 modules labeled with different colors. (b) Heat map showing module-flavor correlations. Each column corresponds to a module indicated by different colors. Each row corresponds to a flavor compound. Red color indicates a positive correlation between the cluster and the tissue. Blue color indicates a negative correlation.

pathway, which takes fatty acids as substrates to produce esters, might be a possible pathway leading to the synthesis of ethyl butanoate and methyl butanoate in kiwifruit. The screening of the structural genes involved in the β-oxidation pathway in the blue module identified 13 genes as good candidates encoding key enzymes in the biosynthesis pathway of ethyl butanoate and methyl butanoate, including four *long-chain acyl-CoA synthetases* (*AcLACS5, AcLACS6.1, AcLACS6.2, AcLACS11*), one *acyl-CoA oxidase* (*AcACX2*), two *multifunctional proteins* (*AcMFP12, AcMFP16*), two *ketoacyl-CoA thiolases* (*AcKAT2.1, AcKAT2.2*), two *alcohol dehydrogenases* (*AcADH1, AcADH2*), and two *alcohol acyltransferases* (*AcAAT10, AcAAT12*) (Fig. 4c; Dataset S8). Further analysis generated a correlation network based on the identification of 86 transcription factors in the blue module whose expression was highly correlated with transcripts of the 13 structural genes and having the potentially the ability to bind the *cis*-elements present in their promoters (Fig. 4c; Dataset S8). Among the 86 transcription factors in the correlation network (Dataset S8), 19 correspond to NAC-type transcription factors, suggesting an important role for the NAC family in modulating ester biosynthesis.

Identification of key transcription factors regulating sugar metabolism

To address the regulatory roles of the key transcription factors potentially controlling flavor metabolism, we selected the regulatory network of soluble sugars considering its major contribution to the buildup of flavor quality of kiwifruit. Since starch degradation is one of the most important sources for sugar accumulation

during kiwifruit ripening, we focused our analysis on the regulatory network of α-amylase (*AMY*) and β-amylase (*BAM*) genes which play a key role in the switch from starch to soluble sugars accumulation during ripening of kiwifruit. Among the 21 structural genes (Fig. 4a), six *α-amylases* (*AMY*) and *β-amylase* (*BAM*) genes were identified as associated with accumulation of soluble sugars during fruit development and ripening. To characterize the key transcription factors modulating activation of the structural genes encoding enzymes of soluble sugar accumulation, we focused on the regulation of *AcBAM3.5* because this structural gene displayed the highest transcript accumulation and expression specificity among the 21 soluble sugar metabolic-related genes during fruit ripening (Dataset S6). The regulatory network analysis indicated that *AcBAM3.5* transcripts are highly correlated with 43 transcription factors including ERF, NAC, MYB and bHLH families (Fig. 5a; Dataset S6). Because *AcBAM3.5* was shown previously to strongly respond to the ripening hormone ethylene (Gunaseelan *et al.*, 2019), we investigated the regulation of *AcBAM3.5* by the ERF-type transcription factors since ERFs are known as the direct mediators of ethylene responsive genes (Pirrello *et al.*, 2012). The correlation between *AcBAM3.5* transcripts and the relative expression levels during fruit development and ripening, pointed to AcERF182 as a best candidate transcription factor for further study (Fig. 5b; Dataset S6).

To investigate the potential regulatory effect of AcERF182 on *AcBAM3.5*, we carried out an *in silico* search of typical regulatory motifs in the *AcBAM3.5* promoter sequence, which revealed the presence of conserved DRE/CRT *cis*-elements known to be the putative binding sites of the ERF-type transcription factors
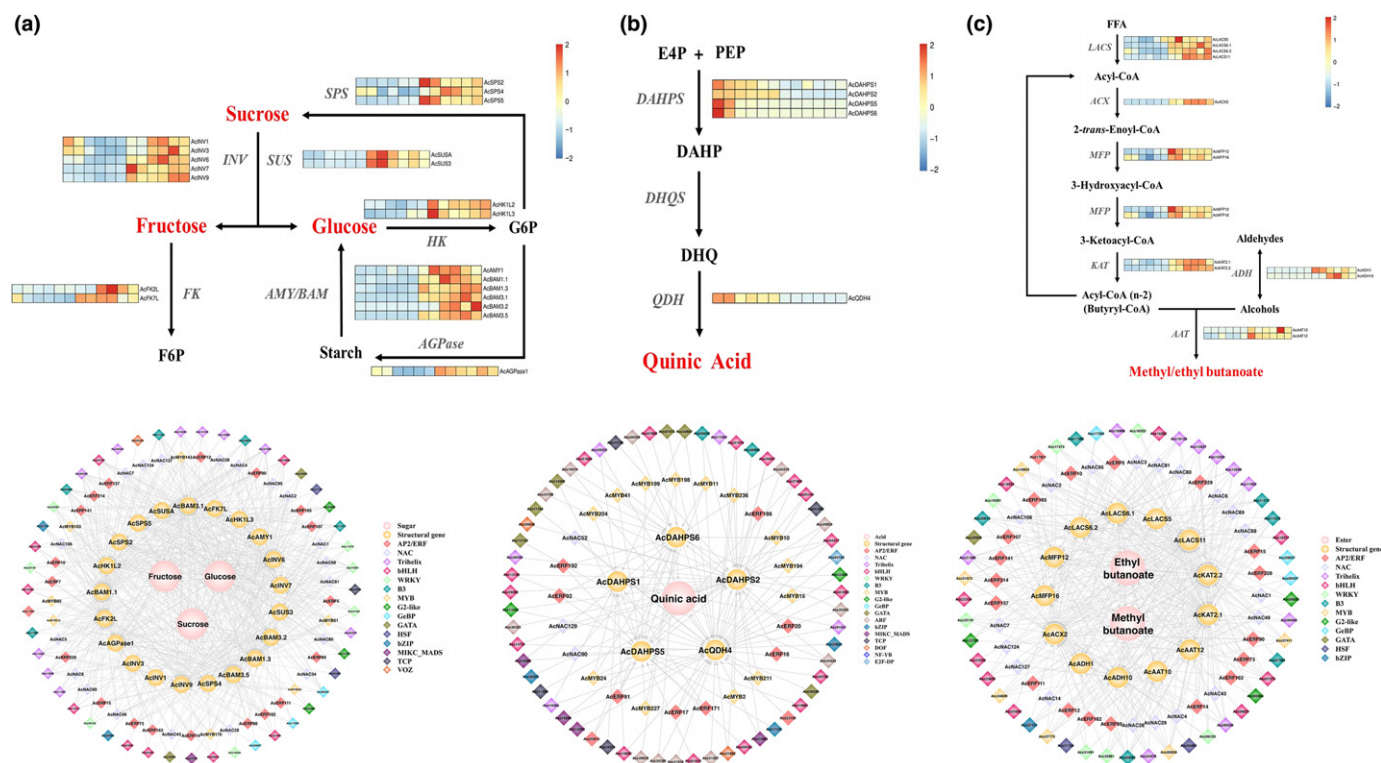
Fig. 4 The regulatory network of key flavor metabolites in kiwifruit. (a) Upper: metabolic pathway for soluble sugars and putative transcriptional regulatory network. INV, invertase; SUS, sucrose synthase; HK, hexokinase; AMY/BAM, α-/β-amylases; FK, fructokinase; AGPase, ADP glucose pyrophosphorylase; SPS, sucrose phosphate synthetase. (a) Lower: pink circles represent soluble sugars. Yellow circles represent structural genes involved in soluble sugars metabolism during fruit development and ripening. Diamonds with different colors represents different families of transcription factors identified in the same module whose transcripts are correlated with expression of structural genes. (b) Upper: quinic acid metabolic pathway and putative transcriptional regulatory network. DAHPS, 3-deoxy-D-arabino-heptulosonate 7-phosphate synthase; DHQS, 3-dehydroquinate synthase; QDH, quinate dehydrogenase. (b) Lower: pink circles represent quinic acid. Yellow circles represent structural genes involved in quinic acid biosynthesis. Diamonds with different colors represents different families of transcription factors identified in the same module whose transcripts are correlated with expression of structural genes. (c) Upper: ethyl butanoate and methyl butanoate metabolic pathway and putative transcriptional regulatory network. LACS, long-chain acyl-CoA synthetase; ACX, acyl-CoA oxidase; MFP, multifunctional protein; KAT, ketoacyl-CoA thiolase; ADH, alcohol dehydrogenase; AAT, alcohol acyltransferase. (c) Lower: pink circles represent ethyl butanoate and methyl butanoate. Yellow circles represent structural genes involved in ethyl butanoate and methyl butanoate metabolism. Diamonds with different colors represents different families of transcription factors identified in the same module whose transcripts are correlated with expression of structural genes.

(Supporting Information Fig. S1a). Dual luciferase reporter assays were carried out by co-transfecting protoplasts with reporter and effector constructs to assess the effect of AcERF182 on the promoter activity of *AcBAM3.5*. A DNA fragment (1822 bp) corresponding to the promoter region of *AcBAM3.5* harboring the DRE/CRT box was fused to the firefly luciferase (LUC) coding sequence to generate the dual luciferase reporter plasmid with renilla luciferase (REN) reporter driven by the 35S promoter as an internal control. Co-expression of *p35S::AcERF182* effector with the *proAcBAM3.5:: LUC* in protoplasts isolated from *Nicotiana benthamiana* leaves resulted in a significant increase in luminescence intensity (Fig. 5c), revealing the ability of AcERF182 to regulate the transcription of *AcBAM3.5 in vivo*. To further investigate the capacity of AcERF182 to directly bind the *AcBAM3.5* promoter, we expressed AcERF182 fused to the GAL4 AD in a Y1H system to challenge it with the *AcBAM3.5* promoter fused to the HIS2 reporter. The induction effect of AcERF182 on yeast growth compared to the control indicated that AcERF182 is able to induce the *AcBAM3.5* promoter activity via the DRE/CRT *cis*-element (Fig. 5d). Consistently,

EMSAs indicated that AcERF182 directly binds to the DNA probe containing the DRE/CRT box present in the promoter region of *AcBAM3.5* (Fig. 5e). Altogether, these data support the hypothesis that AcERF182 may play an important role in the accumulation of soluble sugar metabolism via direct regulation of the transcription of *AcBAM3.5* during fruit ripening of kiwifruit.

AcERF182 regulates soluble sugar accumulation in kiwifruit

The activation of AcERF182 on the transcription of *AcBAM3.5* prompted us to investigate the regulation of AcERF182 on soluble sugar accumulation. We therefore generated both overexpression and VIGS constructs targeting the transcription factor *AcERF182* in order to test their ability to impact *in vivo* the accumulation of soluble sugars in kiwifruit. For this purpose, *Agrobacterium tumefaciens* strain GV3101 containing recombinant plasmid *35S:: AcERF182* or *pTRV2::AcERF182* was injected into the fruit of 'Hongyang' at 100 DAP. To enhance the efficacy of the injection, we repeated the injection every 10 d until 140 DAP. The
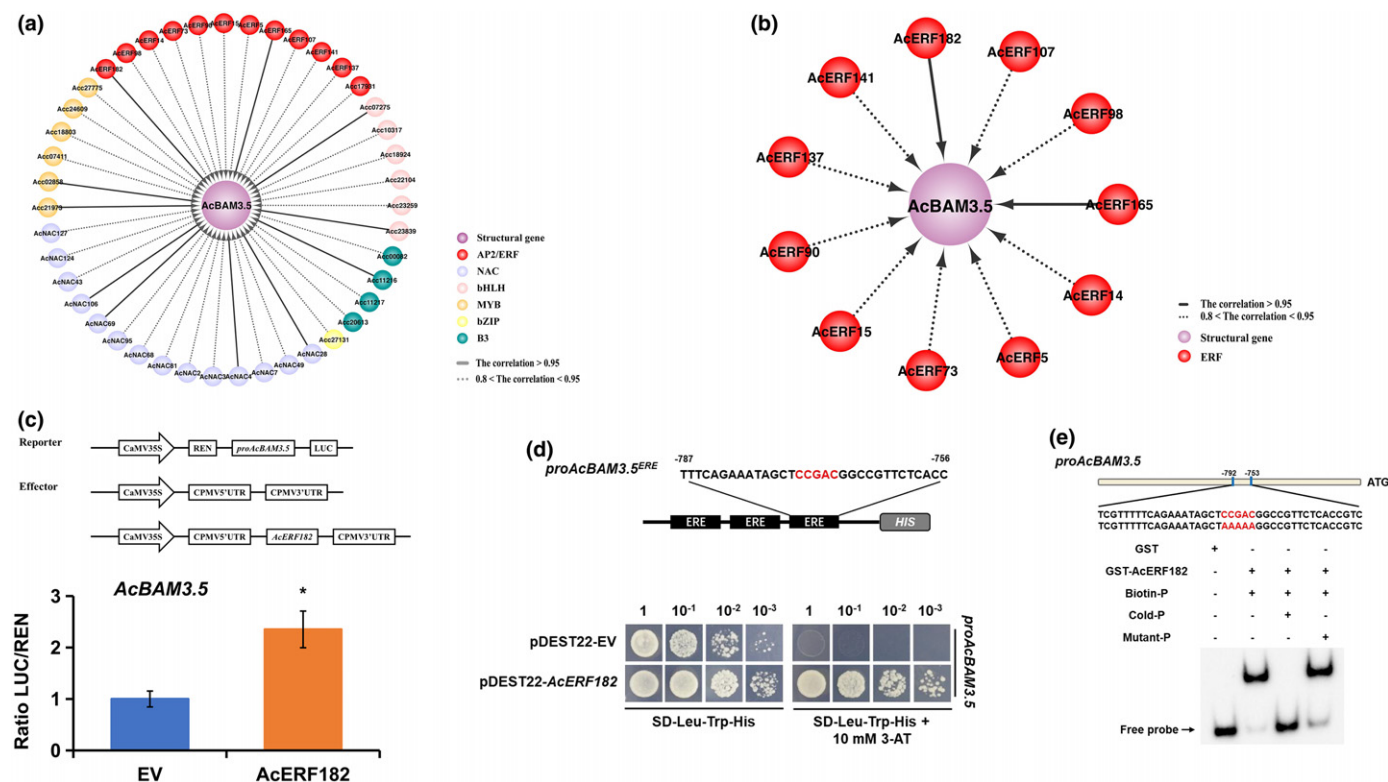
Fig. 5 Identification of AcERF182 as a key transcription factor regulating *AcBAM3.5* in kiwifruit. (a) Transcriptional regulatory network of *AcBAM3.5*. Circles with different colors represents different families of transcription factors (TFs) identified as being highly correlated with *AcBAM3.5*. Solid lines represent correlations higher than 0.95; dotted lines represents correlation between 0.8 and 0.95. (b) Correlation between *AcBAM3.5* and ERF family genes in the same module. Solid lines represent correlations higher than 0.95; dotted lines represents correlation between 0.8 and 0.95. (c) Transcriptional activation of *AcBAM3.5* by AcERF182 and the values shown are the means ± SD, as indicated by transactivation assay. Different combinations of dual LUC/REN reporter and effector plasmids were co-transformed into *Nicotiana benthamiana* leaf protoplasts. Asterisks indicate statistical significance using Student's *t*-test: *, $P < 0.05$. (d) AcERF182 activates *AcBAM3.5* promoter as indicated by yeast one-hybrid assays. Yeast cells were co-transformed with a bait vector, containing *AcBAM3.5* promoter fragment fused to a *HIS2* reporter gene, and a prey vector, containing AcERF182 fused to a GAL4 activation domain. 10 mM 3-AT (3-amino-1,2,4-triazole) was used to suppress background growth and test the strength of the interaction. (e) AcERF182 binding to the promoter of *AcBAM3.5* containing a DRE/CRT element. The wild-type (WT) probe containing the DRE/CRT was biotin-labeled. Competition for AcERF182 binding was performed with cold probes. The symbols − and + represent absence or presence of the probes and GST-tagged AcERF182 protein.

effectiveness of the strategy was validated by RT-qPCR analysis at 140 DAP showing that the relative expression of *AcERF182* was significantly upregulated in the *35S::AcERF182* transient expression fruits and downregulated in fruits infiltrated with the *AcERF182 pTRV2* VIGS construct (Fig. 6a). Interestingly, the sucrose, fructose, and glucose contents were all significantly increased in the *AcERF182* overexpressing fruits while decreased in the silenced lines (Fig. 6b), confirming a direct regulation of AcERF182 on soluble sugar metabolism in kiwifruit. Consistent with the high expression levels of *AcERF182* and the accumulation of soluble sugars, the relative expression of *AcBAM3.5* was upregulated in kiwifruit fruits transiently expressing *AcERF182* (Fig. 6c). Conversely, *AcBAM3.5* was downregulated in VIGS fruits (Fig. 6c).

Identification of a key transcription factor regulating ester metabolism

To investigate the regulation of the synthesis of the two key esters (ethyl butanoate and methyl butanoate) in kiwifruit, we selected *alcohol acyltransferase* (*AcAAT10*) as candidate structural genes from the regulatory network since AATs act directly in the formation of esters. Because *AcAAT10* displayed a significantly higher expression correlation with ethyl butanoate and also a significantly higher expression level during fruit ripening compared to *AcAAT12* (Dataset S8), we focused our studies on the transcriptional regulation of *AcAAT10*. Of the six transcription factors whose transcript accumulation was positively correlated with *AcAAT10* in the regulatory network, a NAC transcription factor AcNAC4 was the most highly expressed (Fig. 7a; Dataset S8), suggesting that AcNAC4 may act as a key regulator in ester biosynthesis by regulating the transcription of *AcAAT10*.

AcNAC4 regulates the transcription of *AcAAT10* by binding to and activating its promoter

To investigate whether AcNAC4 is able to regulate the transcription of *AcAAT10*, we performed dual luciferase reporter assays in tobacco protoplasts using *35S::AcNAC4* as effector and *proAcAAT10::LUC* as reporter. The results showed that co-
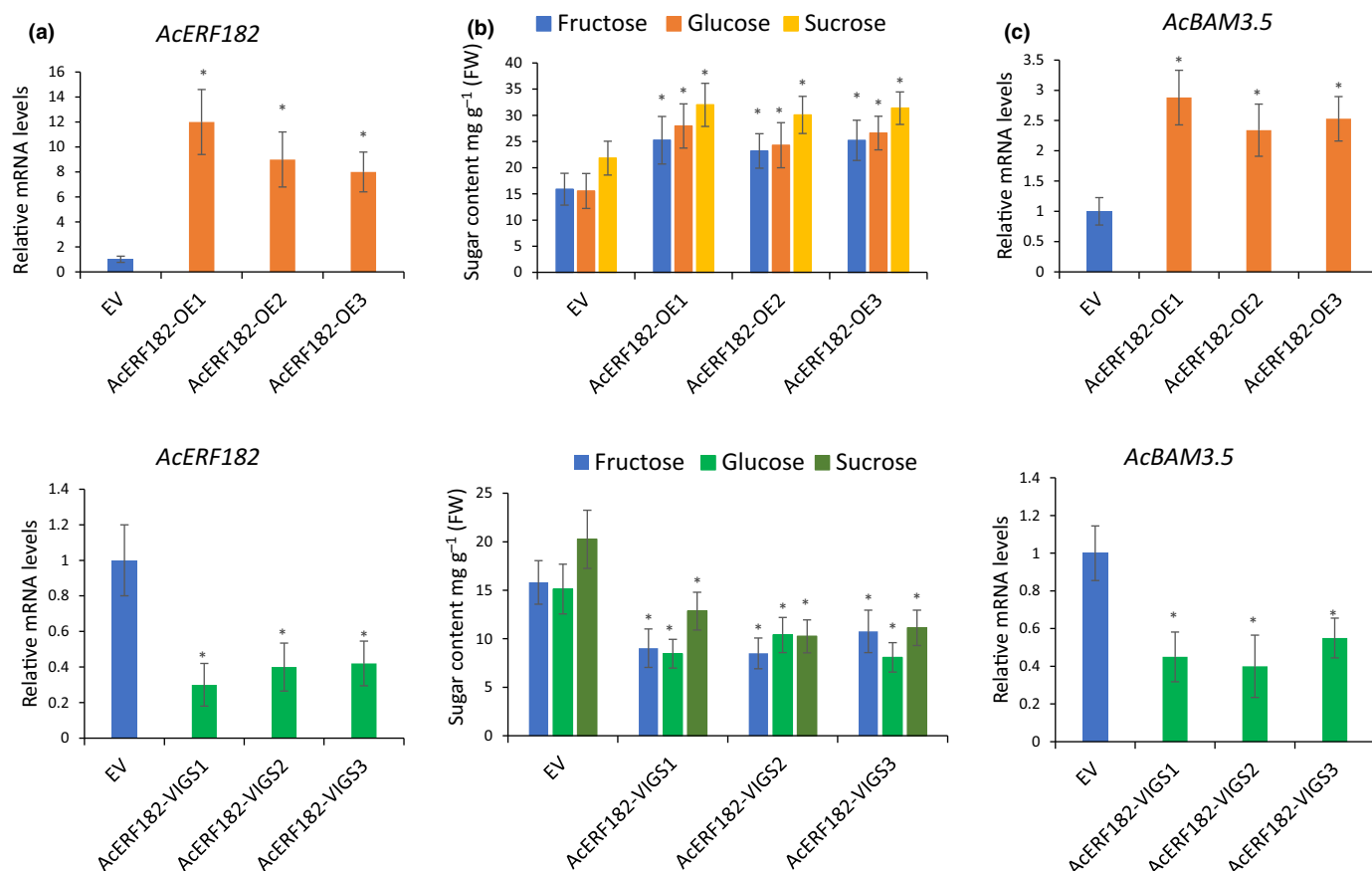
Fig. 6 AcERF182 modulates sugar accumulation by regulation of *AcBAM3.5* in kiwifruit. (a) Relative mRNA levels of *AcERF182* in *AcERF182* overexpression and virus-induced gene silencing lines and the values shown are the means ± SD, as assessed by real-time quantitative polymerase chain reaction (RT-qPCR). EV, empty vector. *AcERF182*-OE1, *AcERF182*-OE2 and *AcERF182*-OE3 are three independent *AcERF182* overexpression lines. *AcERF182*-VIGS1, *AcERF182*-VIGS2 and *AcERF182*-VIGS3 are three independent *AcERF182* silencing lines. Asterisks indicate statistically significant differences using Student's *t*-test: *, $P < 0.05$. (b) Fructose, glucose, sucrose contents in *AcERF182* overexpression and virus-induced gene silencing lines and the values shown are the means ± SD. EV, empty vector. *AcERF182*-OE1, *AcERF182*-OE2 and *AcERF182*-OE3 are three independent *AcERF182* overexpression lines. *AcERF182*-VIGS1, *AcERF182*-VIGS2 and *AcERF182*-VIGS3 are three independent *AcERF182* silencing lines. Asterisks indicate statistical significance using Student's *t*-test: *, $P < 0.05$. (c) Relative mRNA levels of *AcBAM3.5* in *AcERF182* overexpression and virus-induced gene silencing lines and the values shown are the means ± SD, as assessed by real-time quantitative polymerase chain reaction (RT-qPCR). Asterisks indicate statistically significant differences using Student's *t*-test: *, $P < 0.05$.

expression of the effectors with the reporter constructs significantly induced the activity of the *AcAAT10* promoter compared to the control (Fig. 7b), indicating the positive regulation of the *AcAAT10* promoter by AcNAC4. Moreover, both Y1H and EMSA confirmed the binding of AcNAC4 to the *cis*-elements in the promoter region of *AcAAT10* (Fig. 7c,d). Taken together, these results demonstrated that the transcription factor AcNAC4 regulates the expression of *AcAAT10* through directly binding the core sequence (ACGTA) present in the *AcAAT10* promoter regions.

AcNAC4 controls ester biosynthesis in *Actinidia chinensis* cv. Hongyang

To examine the impact of AcNAC4-dependent regulation on the biosynthesis of ethyl butanoate and methyl butanoate, we generated both *AcNAC4* overexpression and VIGS constructs as described earlier. Transient overexpression or silencing of *AcNAC4* was then conducted by injection of *Agrobacterium tumefaciens* strain GV3101

containing recombinant plasmid *35S::AcNAC4* or *pTRV2:: AcNAC4* into the fruit of 'Hongyang' at 100 DAP. After harvest at 140 DAP, the content of both ethyl butanoate and methyl butanoate was significantly increased in the *AcNAC4* overexpressing fruits compared with the control while it was decreased in the silencing lines (Fig. 8a). Consistently, *AcNAC4* and *AcAAT10* transcript levels were higher in overexpressing fruits and lower in the silenced lines (Fig. 8b,c). The data indicated that AcNAC4 plays an important role in modulating ethyl butanoate and methyl butanoate biosynthesis via regulating the expression of key gene *AcAAT10* encoding an alcohol acetyltransferase.

Regulation of flavor metabolism by key transcription factors revealed in different kiwifruit varieties

The data described earlier regarding the role of transcription factors in regulating flavor metabolism were all obtained with *Actinidia chinensis* cv Hongyang, which raises the question whether they
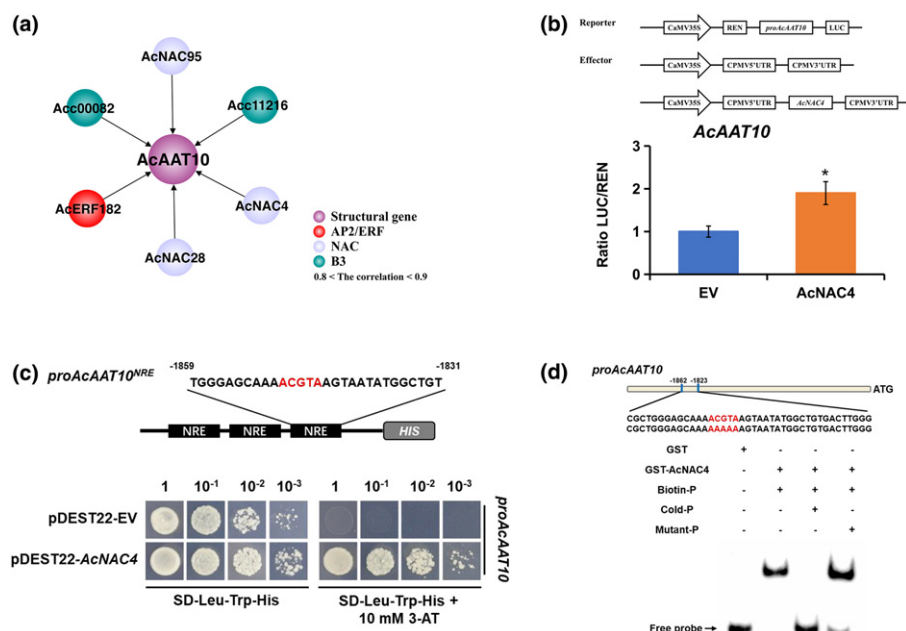
Fig. 7 Identification of transcription factor AcNAC4 as a key regulator modulating *AcAAT10* in kiwifruit. (a) Transcriptional regulatory network for *AcAAT10*. Circles with different colors represents different families of transcription factors identified as being highly correlated with *AcAAT10*. (b) Transcriptional activation of *AcAAT10* by AcNAC4 as indicated by transactivation assay and the values shown are the means ± SD. Different combinations of dual LUC/REN reporter and effector plasmids were co-transformed into *Nicotiana benthamiana* leaf protoplasts. Asterisk indicates statistically significant differences using Student's *t*-test: *, $P < 0.05$. (c) AcNAC4 activates the *AcAAT10* promoter as indicated by yeast one-hybrid assays. Yeast cells were co-transformed with a bait vector, containing an *AcAAT10* promoter fragment fused to a *HIS2* reporter gene, and a prey vector, containing AcNAC4 fused to a GAL4 activation domain. 10 mM 3-AT (3-amino-1,2,4-triazole) was used to suppress background growth and test the strength of the interaction. (d) AcNAC4 binding to the promoter of *AcAAT10*. The wild-type (WT) probe containing the NAC binding site was biotin-labeled. Competition for AcNAC4 binding was performed with cold probes. The symbols − and + represent absence or presence of the probes and GST-tagged AcNAC4 protein.

are valid for all other kiwifruit cultivars. To address this issue, we examined the correlation between the content of soluble sugars, key esters and the expression levels of key transcription factor in four other kiwifruit varieties, namely *Hongyang, Hongshi, Hort16A,* and *Actinidia arguta*. The results showed that all four varieties contain high levels of sucrose, fructose, and glucose at the edible ripening stage compared to the harvest stage (Fig. 9a). Interestingly, the expression levels of the key transcription factor AcERF182 were highly correlated with the sugar accumulation at both harvest ripe and eating ripe stages in all varieties examined (Fig. 9b). Moreover, in line with the accumulation pattern of sugar, *AcERF182* and *AcBAM3.5* also displayed a relatively high expression level at the edible ripe stage in the four varieties (Fig. 9c). These results support the notion that the active role of AcERF182 in regulating the key structural gene *AcBAM3.5* involved in soluble sugar accumulation is conserved in different varieties of kiwifruit. Moreover, the contents of ethyl butanoate and methyl butanoate, two key esters in most kiwifruit varieties, were also highly correlated with the expression levels of *AcNAC4* and *AcAAT10* in all varieties tested (Fig. 9d,e). Overall, our findings confirmed that the flavor regulatory network is a useful dataset for the identification of key transcription factors that modulate flavor metabolism in kiwifruit.

Discussion

Elucidating the metabolic pathways and regulators governing the synthesis and accumulation of key flavor compounds is essential

in order to provide new leads for improving fruit flavor quality. As illustrated by our study, the comprehensive analysis of flavor-related metabolome and transcriptome at different stages of development and ripening of kiwifruit enabled the generation of regulatory networks associated with the accumulation of key flavor components. Using our datasets, we identified key transcription factors that regulate the metabolism of soluble sugars including sucrose, fructose and glucose and also esters such as ethyl butanoate and methyl butanoate and revealed their role in modulating the transcription of the key structural genes involved in these metabolic pathways. The datasets generated can be further used to identify the key structural and regulatory genes involved in flavor-related metabolism. This not only helps to define the regulatory networks controlling specific flavor compounds, but also opens up new avenues for future breeding strategies aimed at improving kiwifruit quality. Overall, the new information gained here in the field of the molecular basis of kiwifruit flavor provides a compelling example of a roadmap for the analysis of flavor regulation analysis in other fruit species.

The dataset provides a useful resource towards the clarification of the metabolic pathways of key flavor compounds not yet deciphered in kiwifruit. Combining these transcriptomic and metabolomic resources allow the identification of key structural and regulatory genes involved in flavor-related metabolism in kiwifruit. Ethyl butanoate and methyl butanoate are two main volatiles contributing to the fruity aroma of ripe fruit of different species of kiwifruit (Paterson *et al.*, 2010;
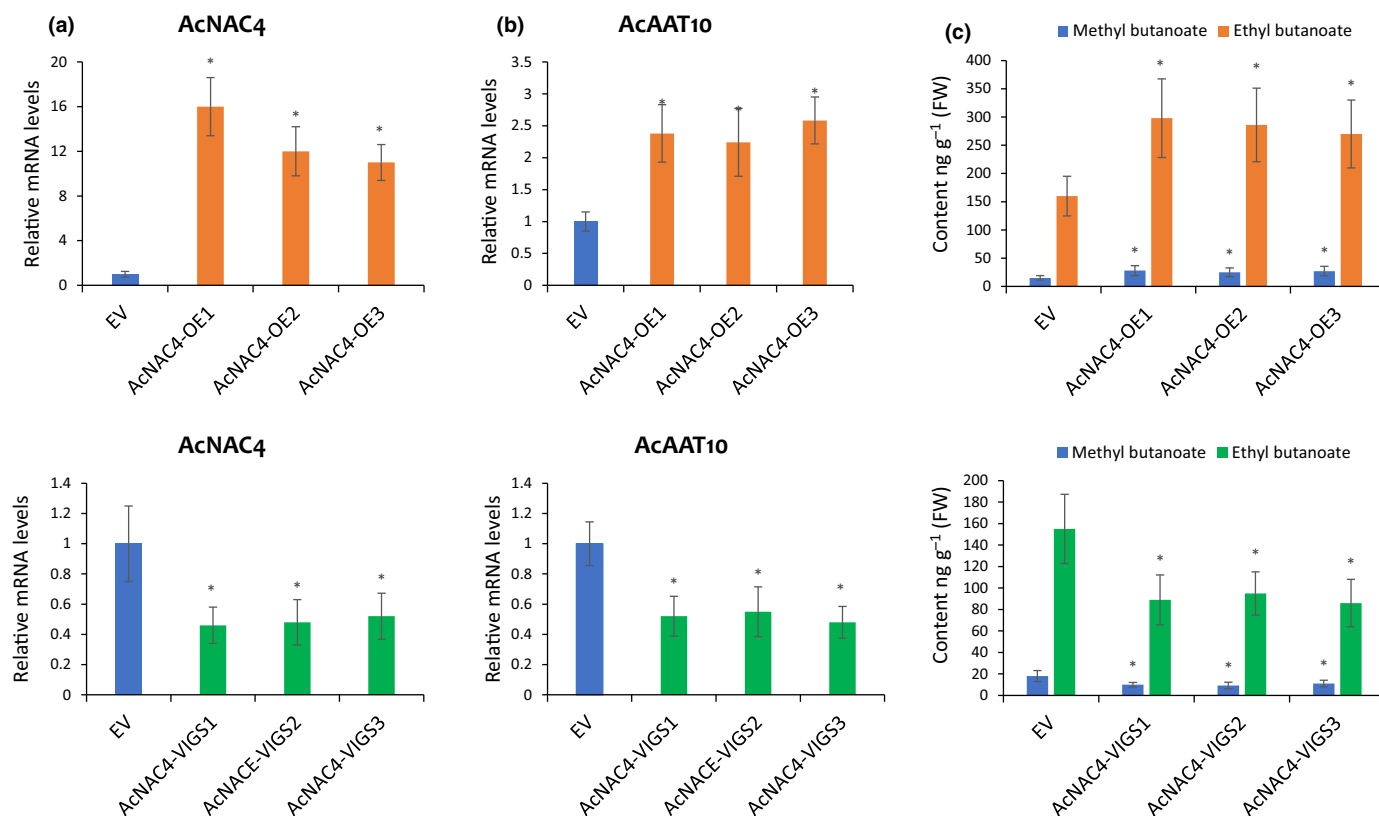
Fig. 8 Transcription factor AcNAC4 modulates ester accumulation by regulation of *AcAAT10* in kiwifruit. (a) Relative mRNA levels of *AcNAC4* in *AcNAC4* overexpression and virus-induced gene silencing lines and the values shown are the means ± SD, as assessed by real-time quantitative polymerase chain reaction (RT-qPCR). EV, empty vector. *AcNAC4*-OE1, *AcNAC4*-OE2 and *AcNAC4*-OE3 are three independent *AcNAC4* overexpression lines. *AcNAC4*-VIGS1, *AcNAC4*-VIGS2 and *AcNAC4*-VIGS3 are three independent *AcNAC4* virus-induced gene silencing lines. Asterisks indicate statistically significant differences using Student's *t*-test: *, *P* < 0.05. (b) Relative mRNA levels of *AcAAT10* in *AcNAC4* overexpression and virus-induced gene silencing lines and the values shown are the means ± SD, as assessed by RT-qPCR. Asterisks indicate statistical significance using Student's *t*-test: *, *P* < 0.05. (c) Ethyl butanoate and methyl butanoate contents in *AcNAC4* overexpression and the values shown are the means ± SD. EV, empty vector. *AcNAC4*-OE1, *AcNAC4*-OE2 and *AcNAC4*-OE3 are three independent *AcNAC4* overexpression lines. *AcNAC4*-VIGS1, *AcNAC4*-VIGS2 and *AcNAC4*-VIGS3 are three independent *AcNAC4* silencing lines. Asterisks indicate statistically significant differences using Student's *t*-test: *, *P* < 0.05.

Souleyre *et al.*, 2010; Wang *et al.*, 2011). Previous studies focused mainly on the identification of AATs that belong to the BAHD acyltransferase superfamily acting at the final step in ester biosynthesis and investigation of the effect of modulating key AATs in ester biosynthesis in different kiwifruit species (Crowhurst *et al.*, 2008; Souleyre *et al.*, 2010; Gunther *et al.*, 2011; Mitalo *et al.*, 2019; Zhang *et al.*, 2020). However, to date, the detailed metabolic pathway of the two key esters in kiwifruit remains largely unclear. Through analysis of the putative structural genes in the blue module (Fig. 4c), associated with ethyl butanoate and methyl butanoate metabolism, we identified that ethyl butanoate and methyl butanoate might be derived from free fatty acids (FFAs) through the β-oxidation pathway and identified key structural genes involved in different steps of this metabolic pathway. Subsequently, we identified key transcription factors that modulate the biosynthesis of the two esters by regulating the expression of associated key structural genes.

Our dataset, not only allows to verify some previously reported metabolic regulatory network information but also allows the identification of novel transcription factors that regulate the accumulation of flavor components in kiwifruit. Previous studies

involving transcriptome analysis in kiwifruit (Zhang *et al.*, 2018) have identified a zinc finger transcription factor AdDof3 that regulates starch degradation and soluble sugar accumulation via regulating the transcription of *AdBAM3L* (β-amylase) (*Actinidia deliciosa*). In our dataset, we verified the relatively high expression correlation ($r = 0.74$) between the homolog of *AdDof3* (i.e. *AcDof3*) and the homolog of *AdBAM3L* (i.e. *AcBAM3.5*), suggesting that our dataset is a reliable resource to identify regulators that control flavor metabolism. Nevertheless, the expression correlation ($r = 0.96$) between *AcERF182* and *AcBAM3.5* is significantly higher than that between *AcDof3* and *AcBAM3.5*, and considering the much higher expression levels of *AcERF182* throughout fruit development and ripening, we proposed that AcERF182 might be a key regulator that modulates starch degradation and soluble sugar accumulation. This assertion is supported by the demonstrated transcriptional regulatory action of AcERF182 on *AcBAM3.5* revealed by transcriptional activation, Y1H, EMSA and transient expression assays. Moreover, our data also confirmed the high negative correlation ($r = -0.93$) between the homolog of *AdDof4* and homolog of *AdFAD1* (Dataset S9) that was recently reported to be negatively correlated and to play
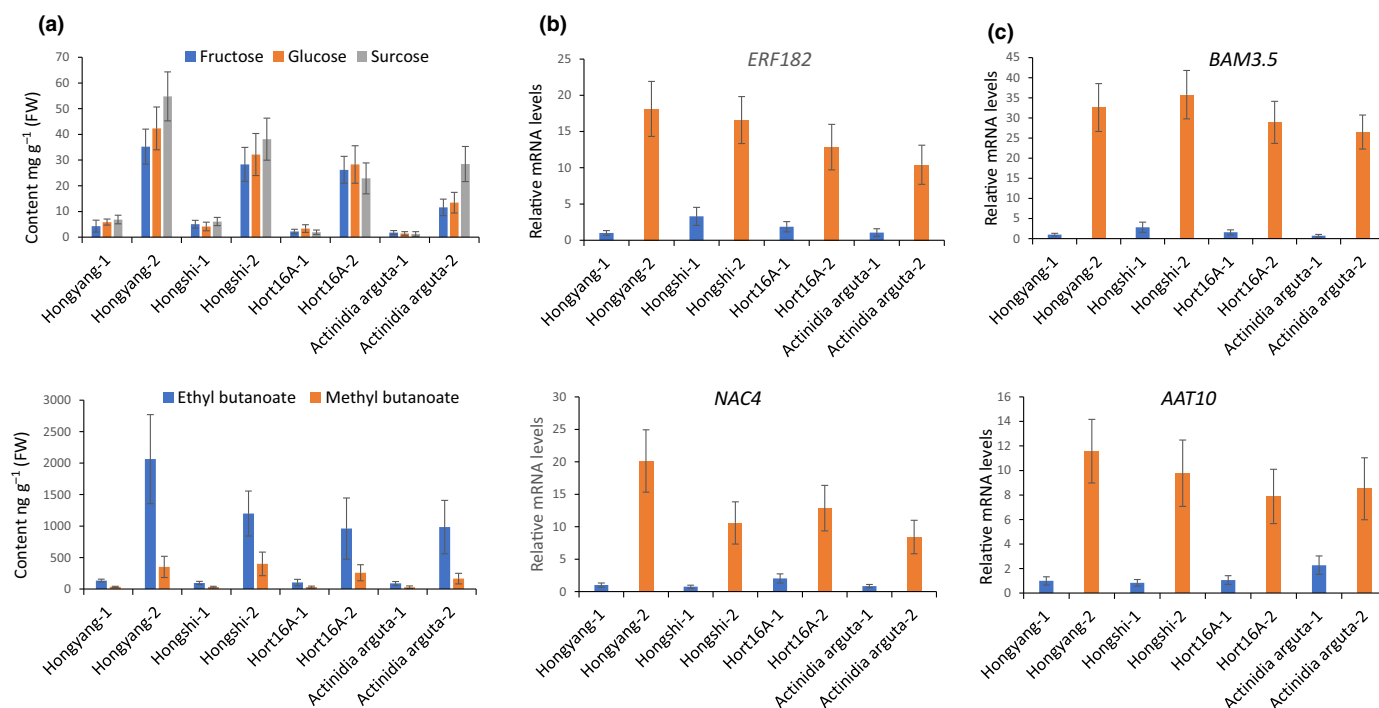
Fig. 9 Regulatory effect of transcription factors on flavor metabolism in different kiwifruit varieties. (a) Fructose, glucose, sucrose contents in different kiwifruit varieties and the values shown are the means ± SD. *Hongyang*, *Hongshi*, *Hort16A* and *Actinidia arguta* are four different kiwifruit varieties. 1, represents harvest stage; 2, represents edible ripening stage. (b, c) Relative mRNA levels of *AcERF182* and *AcBAM3.5* in different kiwifruit varieties and the values shown are the means ± SD, as assessed by real-time quantitative polymerase chain reaction (RT-qPCR). (d) Ethyl butanoate and methyl butanoate contents in different kiwifruit varieties and the values shown are the means ± SD. (e, f) Relative mRNA levels of *AcNAC4* and *AcAAT10* in different kiwifruit varieties and the values shown are the means ± SD, as assessed by RT-qPCR.

an important role in ester biosynthesis (Zhang *et al.*, 2020). In addition to validating the previously reported regulation of flavor metabolism, our dataset can also be used to verify the regulation of transcription factors during other developmental processes such as fruit ripening. Wang *et al.* (2020) showed that AdNAC6 and AdNAC7 play an important role in regulating ripening-related genes such as *AdACS1*, *AdACO1* and *AdMAN1*. Concordantly, our dataset revealed a high correlation between *AdNAC6* and *AdNAC7* transcript levels with transcript levels of the same ripening-related genes (Dataset S9). All these findings suggest that our dataset is a useful resource for understanding more broadly the transcriptional regulation of important processes in kiwifruit.

The *NAC* gene family is one of the largest transcription factor families in plants shown to be involved in leaf senescence and fruit ripening (Giovannoni, 2004; Guo & Gan, 2006; Uauy *et al.*, 2006; Gao *et al.*, 2018; Ma *et al.*, 2018). In particular, *NAC* genes have been extensively studied with regards to their role during kiwifruit ripening. AaNAC2-4 were shown to control monoterpene production by regulating the terpene synthase gene (*AaTPS1*) during *Actinidia arguta* fruit ripening (Nieuwenhuizen *et al.*, 2015). AdNAC5 has been reported to regulate the expression of *AdFAD1* which acts as a structural gene of ester biosynthesis (Zhang *et al.*, 2018). It was also shown that AdNAC2/3 are involved in fruit ripening via physically interacting with and trans-activating the *AdACS1* promoter (Wu *et al.*, 2020). More recently, AdNAC2 and AdNAC72 have been shown to bind directly to the promoter of *AdMsrB1* to increase free methionine and ethylene

production during kiwifruit ripening (Fu *et al.*, 2021). Interestingly, AcNAC4 identified in our study as part of the regulatory network of ethyl butanoate and methyl butanoate metabolism was shown to directly regulate the *AcAAT* gene (*AcAAT10*) in kiwifruit leading to the accumulation of ethyl butanoate and methyl butanoate. In this regard, our finding uncovers a role and mode of action of NAC-type transcription factors in regulating kiwifruit fruit flavor different from those reported so far.

Quinic acid, produced from dehydroquinate via the enzyme QDH, is one of the main organic acids present in fruit of different kiwifruit species (Nishiyama *et al.*, 2008; Marsh *et al.*, 2009; Jiang *et al.*, 2020). Although QDH has been known to act at the last step to regulate the biosynthesis of quinic acid, to date, very few *QDH* genes have been identified in plants (Guo *et al.*, 2014; Gritsunov *et al.*, 2018). Here, we identified one *QDH* gene (*AcQDH4*) from the turquoise module (Fig. 4c) whose transcript levels are highly correlated with quinic acid metabolism during the processes of fruit development and ripening in kiwifruit. Further studies of the regulatory network of quinic acid metabolism, identified 11 transcription factors that are highly correlated with *AcQDH4* ($r > 0.95$) (Fig. S2; Dataset S7). Among these transcription factors, AcMYB211 showed the highest expression correlation, high expression levels, and the ability to bind to the promoter of *AcQDH4* (Dataset S7). This transcriptional regulator was therefore selected as the putative key regulator controlling quinic acid biosynthesis via regulation of the transcription of *AcQDH4*. The physiological function of AcQDH4 and

AcMYB211 in quinic acid metabolism and the transcriptional regulation of AcMYB12 on *AcQDH4* require further study.

Author contributions

ML planned and designed the research. RW, BZ, CZ and YC performed experiments. PS, JZ, Yaoxin Zhang, KD, YX, ML, TM, Yang Zhang, ZL, JP, KC and BZ analyzed data. ML wrote the manuscript, MB and BZ revised the manuscript and DG helped improve the manuscript. RW, PS and CZ contributed equally to this work.

ORCID

Mondher Bouzayen (iD) https://orcid.org/0000-0001-7630-1449
Don Grierson (iD) https://orcid.org/0000-0002-2238-8072
Zhengguo Li (iD) https://orcid.org/0000-0001-7019-2560
Mingchun Liu (iD) https://orcid.org/0000-0001-8004-1758
Tao Ma (iD) https://orcid.org/0000-0002-7094-6868
Bo Zhang (iD) https://orcid.org/0000-0001-8181-9111
Yang Zhang (iD) https://orcid.org/0000-0002-7793-1108

References

Atkinson R, Gunaseelan K, Wang M, Luo L, Wang T, Norling C, Johnston S, Maddumage R, Schröder R, Schaffer R. 2011. Dissecting the role of climacteric ethylene in kiwifruit (*Actinidia chinensis*) ripening using a 1-aminocyclopropane-1-carboxylic acid oxidase knockdown line. *Journal of Experimental Botany* 62: 3821–3835.

Carrari F, Baxter C, Usadel Björn, Urbanczyk-Wochniak E, Zanor M-I, Nunes-Nesi A, Nikiforova V, Centero D, Ratzka A, Pauly M *et al.* 2006. Integrated analysis of metabolite and transcript levels reveals the metabolic shifts that underlie tomato fruit development and highlight regulatory aspects of metabolic network behavior. *Plant Physiology* 142: 1380–1396.

Crowhurst RN, Gleave AP, MacRae EA, Ampomah-Dwamena C, Atkinson RG, Beuning LL, Bulley SM, Chagne D, Marsh KB, Matich AJ *et al.* 2008. Analysis of expressed sequence tags from *Actinidia*: applications of a cross species EST database for gene discovery in the areas of flavor, health, color and ripening. *BMC Genomics* 9: 351.

Deng H, Pirrello J, Chen Y, Li N, Zhu S, Chirinos X, Bouzayen M, Liu Y, Liu M. 2018. A novel tomato F-box protein, SlEBF3, is involved in tuning ethylene signaling during plant development and climacteric fruit ripening. *The Plant Journal* 95: 648–658

Fu B, Wang W, Liu X, Duan X, Allan A, Grierson D, Yin X. 2021. An ethylene-hypersensitive methionine sulfoxide reductase regulated by NAC transcription factors increases methionine pool size and ethylene production during kiwifruit ripening. *New Phytologist* 232: 236–250.

Fung R, Langenk-Mper G, Gardner RC, Macrae E. 2003. Differential expression within an SPS gene family. *Plant Science* 164: 459–470.

Gao Y, Wei W, Zhao X, Tan X, Fan Z, Zhang Y, Jing Y, Meng L, Zhu B, Zhu H *et al.* 2018. A NAC transcription factor, NOR-like1, is a new positive regulator of tomato fruit ripening. *Horticulture Research* 5: 75.

Garcia C, Quek S, Stevenson R, Winz R. 2011. Characterization of the bound volatile extract from baby kiwi (*Actinidia arguta*). *Journal of Agricultural and Food Chemistry* 59: 8358–8365.

Giovannoni J. 2004. Genetic regulation of fruit development and ripening. *The Plant Cell* S170–180.

Grant C, Bailey T, Noble W. 2011. FIMO: scanning for occurrences of a given motif. *Bioinformatics* 27: 1017–1018.

Gritsunov A, Peek J, Diaz Caballero J, Guttman D, Christendat D. 2018. Structural and biochemical approaches uncover multiple evolutionary trajectories of plant quinate dehydrogenases. *The Plant Journal* 95: 812–822.

Gunaseelan K, McAtee P, Nardozza S, Pidakala P, Wang R, David K, Burdon J, Schaffer R. 2019. Copy number variants in kiwifruit ETHYLENE RESPONSE FACTOR/APETALA2 (ERF/AP2)-like genes show divergence in fruit ripening associated cold and ethylene responses in C-REPEAT/DRE BINDING FACTOR-like genes. *PLoS ONE* 14: e0216120.

Gunther C, Heinemann K, Laing W, Nicolau L, Marsh K. 2011. Ethylene-regulated (methylsulfanyl)alkanoate ester biosynthesis is likely to be modulated by precursor availability in *Actinidia chinensis* genotypes. *Journal of Plant Physiology* 168: 629–638.

Gunther C, Marsh K, Winz R, Harker R, Wohlers M, White A, Goddard M. 2015. The impact of cold storage and ethylene on volatile ester production and aroma perception in 'Hort16A' kiwifruit. *Food Chemistry* 169: 5–12.

Gunther C, Matich A, Marsh K, Nicolau L. 2010. (Methylsulfanyl)alkanoate ester biosynthesis in *Actinidia chinensis* kiwifruit and changes during cold storage. *Phytochemistry* 71: 742–750.

Guo J, Carrington Y, Alber A, Ehlting J. 2014. Molecular characterization of quinate and shikimate metabolism in *Populus trichocarpa*. *The Journal of Biological Chemistry* 289: 23846–23858.

Guo Y, Gan S. 2006. AtNAP, a NAC family transcription factor, has an important role in leaf senescence. *The Plant Journal* 46: 601–612.

Huang S, Ding J, Deng D, Tang W, Sun H, Liu D, Zhang L, Niu X, Zhang X, Meng M *et al.* 2013. Draft genome of the kiwifruit *Actinidia chinensis*. *Nature Communications* 4: 2640.

Jiang Z, Huang Q, Jia D, Zhong M, Tao J, Liao G, Huang C, Xu X. 2020. Characterization of organic acid metabolism and expression of related genes during fruit development of *Actinidia eriantha* 'Ganmi 6'. *Plants* 9: 332.

Jin J, Tian F, Yang D, Meng Y, Kong L, Luo J, Gao G. 2017. PlantTFDB 4.0: toward a central hub for transcription factors and regulatory interactions in plants. *Nucleic Acids Research* 45: D1040–D1045.

Kim D, Langmead B, Salzberg S. 2015. HISAT: a fast spliced aligner with low memory requirements. *Nature Methods* 12: 357–360.

Klee H, Tieman D. 2013. Genetic challenges of flavor improvement in tomato. *Trends in Genetics: TIG* 29: 257–262.

Klee H, Tieman D. 2018. The genetics of fruit flavour preferences. *Nature Reviews. Genetics* 19: 347–356.

Kohl M, Wiese S, Warscheid B. 2011. Cytoscape: software for visualization and analysis of biological networks. *Methods in Molecular Biology* 696: 291–303.

Liao Y, Smyth G, Shi W. 2014. featureCounts: an efficient general purpose program for assigning sequence reads to genomic features. *Bioinformatics* 30: 923–930.

Ma X, Zhang Y, Turečková V, Xue G, Fernie A, Mueller-Roeber B, Balazadeh S. 2018. The NAC transcription factor SlNAP2 regulates leaf senescence and fruit yield in tomato. *Plant Physiology* 177: 1286–1302.

Marsh K, Boldingh H, Shilton R, Laing W. 2009. Changes in quinic acid metabolism during fruit development in three kiwifruit species. *Functional Plant Biology: FPB* 36: 463–470.

Marsh K, Friel E, Gunson A, Lund C, Macrae E. 2006. Perception of flavour in standardised fruit pulps with additions of acids or sugars. *Food Quality and Preference* 17: 376–386.

Mitalo OW, Tokiwa S, Kondo Y, Otsuki T, Galis I, Suezawa K, Kataoka I, Doan AT, Nakano R, Ushijima K *et al.* 2019. Low temperature storage stimulates fruit softening and sugar accumulation without ethylene and aroma volatile production in kiwifruit. *Frontiers in Plant Science* 10: 888.

Moscatello S, Famiani F, Proietti S, Farinelli D, Battistelli A. 2011. Sucrose synthase dominates carbohydrate metabolism and relative growth rate in growing kiwifruit (*Actinidia deliciosa*, cv Hayward). *Scientia Horticulturae* 128: 197–205.

Nardozza S, Boldingh HL, Osorio S, Höhne M, Wohlers M, Gleave AP, MacRae EA, Richardson AC, Atkinson RG, Sulpice R *et al.* 2013. Metabolic analysis of kiwifruit (*Actinidia deliciosa*) berries from extreme genotypes reveals hallmarks for fruit starch metabolism. *Journal of Experimental Botany* 64: 5049–5063.

Nieuwenhuizen N, Chen X, Wang M, Matich A, Perez R, Allan A, Green S, Atkinson R. 2015. Natural variation in monoterpene synthesis in kiwifruit: transcriptional regulation of terpene synthases by NAC and ETHYLENE-INSENSITIVE3-like transcription factors. *Plant Physiology* 167: 1243–1258.

Nishiyama I, Fukuda T, Shimohashi A, Oota T. 2008. Sugar and organic acid composition in the fruit juice of different *Actinidia* varieties. *Food Science & Technology International Tokyo* 14: 67–73.

Osorio S, Alba R, Nikoloski Z, Kochevenko A, Fernie A, Giovannoni J. 2012. Integrative comparative analyses of transcript and metabolite profiles from pepper and tomato ripening and development stages uncovers species-specific patterns of network regulatory behavior. *Plant Physiology* 159: 1713–1729.

Paterson V, Macrae E, Young H. 2010. Relationships between sensory properties and chemical composition of kiwifruit (*Actinidia deliciosa*). *Journal of the Science of Food and Agriculture* 57: 235–251.

Pirrello J, Prasad BCN, Zhang W, Chen K, Mila I, Zouine M, Latché A, Pech JC, Ohme-Takagi M, Regad F *et al.* 2012. Functional analysis and binding affinity of tomato ethylene response factors provide insight on the molecular bases of plant differential responses to ethylene. *BMC Plant Biology* 12: 190.

Richardson Ac, Marsh Kb, Boldingh Hl, Pickering Ah, Bulley Sm, Frearson Nj, Ferguson Ar, Thornber Se, Bolitho Km, Macrae Ea. 2004. High growing temperatures reduce fruit carbohydrate and vitamin C in kiwifruit. *Plant, Cell & Environment* 27: 423–435.

Sanz M, Villamiel M, Martnez-Castro I. 2004. Inositols and carbohydrates in different fresh fruit juices. *Food Chemistry* 87: 325–328.

Souleyre E, Günther C, Wang M, Newcomb R, Marsh KB. 2010. Ester biosynthesis in kiwifruit – from genes to enzymes to pathways. *Acta Horticulturae* 913: 205–211.

Tieman D, Zhu G, Resende M, Lin T, Nguyen C, Bies D, Rambla J, Beltran K, Taylor M, Zhang B *et al.* 2017. A chemical genetic roadmap to improved tomato flavor. *Science* 355: 391–394.

Uauy C, Distelfeld A, Fahima T, Blechl A, Dubcovsky J. 2006. A NAC Gene regulating senescence improves grain protein, zinc, and iron content in wheat. *Science* 314: 1298–1301.

Wang M, Macrae E, Wohlers M, Marsh K. 2011. Changes in volatile production and sensory quality of kiwifruit during fruit maturation in *Actinidia deliciosa* 'Hayward' and *A. chinensis* 'Hort16A'. *Postharvest Biology & Technology* 59: 16–24.

Wang W, Wang J, Wu Y, Li D, Allan A, Yin X. 2020. Genome-wide analysis of coding and non-coding RNA reveals a conserved miR164-NAC regulatory pathway for fruit ripening. *New Phytologist* 225: 1618–1634.

Wu Y, Liu X, Fu B, Zhang Q, Yin X. 2020. Methyl jasmonate enhances ethylene synthesis in kiwifruit by inducing *NAC* genes that activate *ACS1*. *Journal of Agricultural and Food Chemistry* 68: 3267–3276.

Ying S, Su M, Wu Y, Zhou L, Fu R, Li Y, Guo H, Luo J, Wang S, Zhang Y. 2020. Trichome regulator SlMIXTA-like directly manipulates primary metabolism in tomato fruit. *Plant Biotechnology Journal* 18: 354–363.

Zeeman S, Kossmann J, Smith A. 2010. Starch: its metabolism, evolution, and biotechnological modification in plants. *Annual Review of Plant Biology* 61: 209–234.

Zhang A, Wang W, Tong Y, Li M, Grierson D, Ferguson I, Chen K, Yin X. 2018. Transcriptome analysis identifies a zinc finger protein regulating starch degradation in kiwifruit. *Plant Physiology* 178: 850–863.

Zhang A, Zhang Q, Li J, Gong H, Fan X, Yang Y, Liu X, Yin X. 2020. Transcriptome co-expression network analysis identifies key genes and regulators of ripening kiwifruit ester biosynthesis. *BMC Plant Biology* 20: 103.

Zhang B, Tieman D, Jiao C, Xu Y, Chen K, Fei Z, Giovannoni J, Klee H. 2016. Chilling-induced tomato flavor loss is associated with altered volatile synthesis and transient changes in DNA methylation. *Proceedings of the National Academy of Sciences, USA* 113: 12580–12585.

Zhang B, Yin X, Li X, Yang S, Ferguson I, Chen K. 2009. Lipoxygenase gene expression in ripening kiwifruit in relation to ethylene and aroma production. *Journal of Agricultural and Food Chemistry* 57: 2875–2881.

Zhao J, Wei Z, Yang D. 2019. Organizational search, dynamic capability, and business model innovation. *IEEE Transactions on Engineering Management* 68: 785–796.

Supporting Information

Additional Supporting Information may be found online in the Supporting Information section at the end of the article.

Dataset S1 Summary of transcriptome mapping during fruit developmental and ripening stages in kiwifruit.

Dataset S2 Gene expression in 12 different developmental and ripening stages of kiwifruit.

Dataset S3 Genes with averaged TPM ≥ 1 in 12 different developmental and ripening stages of kiwifruit.

Dataset S4 Summary of co-expression gene clusters.

Dataset S5 Summary of co-expression gene modules.

Dataset S6 The regulatory network of soluble sugar metabolism during fruit development and ripening in kiwifruit.

Dataset S7 The regulatory network of quinic acid metabolism during fruit development and ripening in kiwifruit.

Dataset S8 The regulatory network of ester metabolism during fruit development and ripening in kiwifruit.

Dataset S9 Expression and correlation of transcription factors and structural genes reported in previous studies.

Fig. S1 The *cis*-elements presence in the promoters of *AcBAM3.5* and *AcAAT10* genes.

Fig. S2 Correlation between *AcQDH4* and transcription factors in the same module.

Table S1 Primers used in this study.

Please note: Wiley Blackwell are not responsible for the content or functionality of any Supporting Information supplied by the authors. Any queries (other than missing material) should be directed to the *New Phytologist* Central Office.